FA-TR-75087

A GEARLESS SAFE AND ARMING DEVICE FOR ARTILLERY FIRING (PROGRAM SUMMARY AND MATHEMATICAL ANALYSIS)

September 1975

Approved for public release; distribution unlimited.

MUNITIONS DEVELOPMENT AND ENGINEERING DIRECTORATE

U.S. ARMY ARMAMENT COMMAND
FRANKFORD ARSENAL
PHILADELPHIA, PENNSYLVANIA 19137

DISPOSITION INSTRUCTIONS

Destroy this report when it is no longer needed. Do not return it to the originator.

The findings in this report are not to be constued as an official Department of the Army position unless so designated by other authorized documents.

UNCLASSIFIED

SECURITY CLASSIFICATION OF THIS PAGE *(When Data Entered)*

REPORT DOCUMENTATION PAGE

READ INSTRUCTIONS BEFORE COMPLETING FORM

1. REPORT NUMBER: FA-TR-75087	2. GOVT ACCESSION NO.
3. RECIPIENT'S CATALOG NUMBER	
4. TITLE *(and Subtitle)*: A GEARLESS SAFE AND ARMING DEVICE FOR ARTILLERY FIRING (PROGRAM SUMMARY AND MATHEMATICAL ANALYSIS)	5. TYPE OF REPORT & PERIOD COVERED: Final Engineering Report
	6. PERFORMING ORG. REPORT NUMBER
7. AUTHOR(s): LOUIS P. FARACE	8. CONTRACT OR GRANT NUMBER(s)
9. PERFORMING ORGANIZATION NAME AND ADDRESS: FRANKFORD ARSENAL, Attn: SARFA-MDA-E, Philadelphia, PA 19137	10. PROGRAM ELEMENT, PROJECT, TASK AREA & WORK UNIT NUMBERS: AMCMS CODE: 4810.16.4737.7, DA PROJECT: GG27030
11. CONTROLLING OFFICE NAME AND ADDRESS: Commander, Picatinny Arsenal, Dover, NJ 07801	12. REPORT DATE: September 1975
	13. NUMBER OF PAGES: 97
14. MONITORING AGENCY NAME & ADDRESS *(if different from Controlling Office)*	15. SECURITY CLASS. *(of this report)*: UNCLASSIFIED
	15a. DECLASSIFICATION/DOWNGRADING SCHEDULE: N/A

16. DISTRIBUTION STATEMENT *(of this Report)*

Approved for public release; distribution unlimited.

17. DISTRIBUTION STATEMENT *(of the abstract entered in Block 20, if different from Report)*

18. SUPPLEMENTARY NOTES

19. KEY WORDS *(Continue on reverse side if necessary and identify by block number)*

Gearless Safe and Arming Device
Delay Arming Mechanism
Runaway Escapement
Math Model

20. ABSTRACT *(Continue on reverse side if necessary and identify by block number)*

The evaluation of a Gearless Mechanical Safe and Arming Device for Artillery projectiles is described along with design philosophy and analytical models utilized. This device is a large run-away escapement wherein essential mechanical parameters have been adjusted to achieve a relatively low oscillation frequency. The manner in which a serious structural integrity problem was resolved is detailed presenting an analytical basis for miniaturization and weight reduction of devices

DD FORM 1 JAN 73 1473 EDITION OF 1 NOV 65 IS OBSOLETE

UNCLASSIFIED

SECURITY CLASSIFICATION OF THIS PAGE *(When Data Entered)*

20. ABSTRACT (cont)

containing runaway escapements. Ballistic and Rough Handling test results from all phases of this project are included.

TABLE OF CONTENTS

TABLE OF CONTENTS - CONTINUED

TABLE OF CONTENTS - CONTINUED

LIST OF ILLUSTRATIONS

LIST OF ILLUSTRATIONS - CONTINUED

LIST OF TABLES

INTRODUCTION

This program was conducted in Fiscal Years 71 thru 75 as Product Improvement Effort GG 27030 involving PD Fuzes M557 and M739 (previous designation M572E2). This Gearless Safe and Arming (S&A) device was originally submitted in concept as an unsolicited proposal by Delaware Valley Armaments (DVA) Corporation, an M125A1 Booster producer.

The effort which followed resulted in the device pictured in Figure 1 which is 1.314 in. in diameter and .530 in. high such that it can be used in all present and next generation Mechanical Time, Electronic Time, Proximity, and PD fuzing for large caliber spin stabilized weapon systems (90 mm and above).

A structural problem in this device was identified early in Engineering Development Testing as the cause of premature arming of the mechanism in two high-spin weapons. This problem was ultimately eliminated by redesigning the mechanism to run at significantly reduced torque levels.

A dud problem was next encountered with the 8 in. Howitzer Zone 1 charge level - an environment which presents arming problems for all centrifugally driven devices. This problem was ultimately attributed to a combination of factors - the most significant of which was caused by a make shift housing being used on an interim basis; this part maintains the axial separation between the two moving time delay elements. Resolution of various hardware and design descrepancies eventually resulted in a successful ballistic test firing in which 24.5 turn arming delay was demonstrated at high spin together with reliability above 95% at low spin.

It can be concluded from this overall effort that a gearless mechanical safe and arming device for spin stabilized projectiles is technically feasible, can provide arming delay (safe separation) equivalent to mechanical devices containing gear trains (and hobbed pinions), and provide high functioning reliability.

This report is divided into two parts. The first describes the program on a chronological basis giving test results and design rationale where applicable. The second is a discussion of the mechanics of this device in which is included the redesign criteria which played an important part in the overall engineering effort.

M55 DETONATOR

UNARMED POSITION

ARMED POSITION

GEARLESS S & A
ARTILLERY AMMUNITION COMPONENTS DIVISION
FRANKFORD ARSENAL

DESCRIPTION

The function of safe and arming devices is primarily one of lauch safety. A minimum safe separation distance is desired before the device arms the fuze. The way this is traditionally accomplished for zoned weapons, in addition to fixed charge weapons, is to use a double integrating device which yields a fixed arming distance for a particular weapon regardless of projectile muzzle velocity and attendant spin rate. Thus, the device arms in a constant number of turns regardless of spin rate.

Figure 1 shows a top and exploded view of this device. It is essentially a large plate pallet runaway escapement (as opposed to a pin pallet runaway escapement). The rotor and escapewheel functions are combined in one assembly. The pallet lever is not only high in inertia but unbalanced as well. This final factor provides additional arming delay while preserving the double integrating character generally exhibited by runaway escapements powered by a centrifugal gear. In contrast with other S&A devices, it contains no gear and pinion assemblies. This lowers cost and improves mobilization potential. The simplicity and fewer moving parts enhance reliability.

The absence of a gear train significantly reduces the number of escapement half cycles. The thirteen rotor escapewheel teeth yield twenty-three half oscillations of the pallet lever in contrast with the 100 half oscillations of the M125A1 Modular Booster (18:1 gear ratio), and the 250 half oscillations of the M125A1 Alt. Booster (47.25:1 gear ratio). The required time delay must then be acquired through the relatively low frequency of the pallet lever. The manner in which this frequency is determined is discussed in depth in the second part of this report.

The motion of the thirteen escapewheel teeth through the mouth of the pallet lever produces twenty-three half oscillations which take place at a relatively low frequency to provide the arming delay required. Figure 2 shows the contact between the two parts which produces the oscillating motion. The top view characterizes entrance engagement contact (both elements rotate in the same rotational sense) while the bottom view depicts a typical exit engagement contact (lever turns opposite in direction from wheel). The device contains two independent safety systems to sense setback and spin. Given setback without spin or spin without setback the item remains safe. These systems are independent of one another satisfying an important provision of MIL-STD-1316A. The two spin locks comprise one safety system and require a spin level of approximately 1500 rpm to disengage from the rotor gear. The other safety system, the setback pin, is biased such that 17 g's slowly applied axially in the

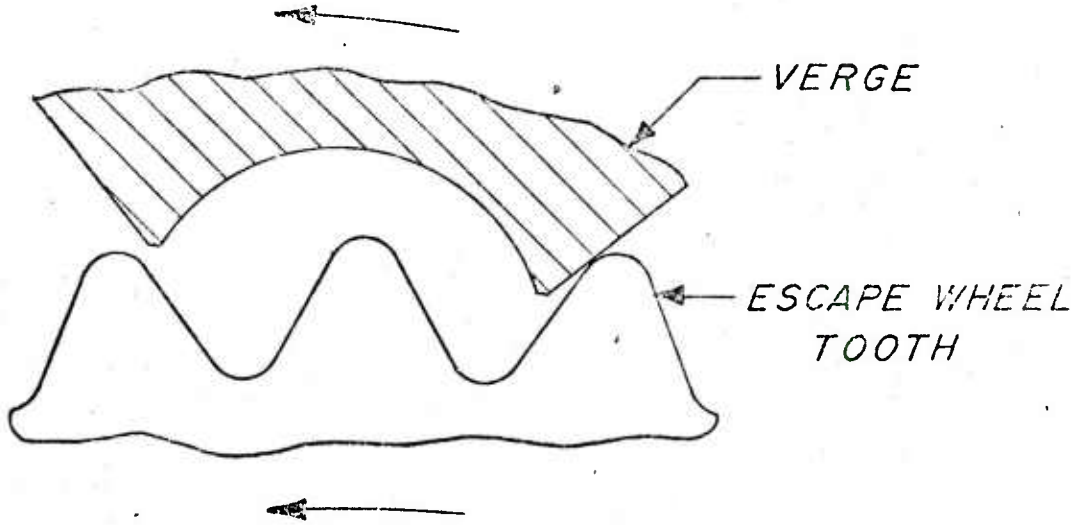

ENTRANCE ENGAGEMENT

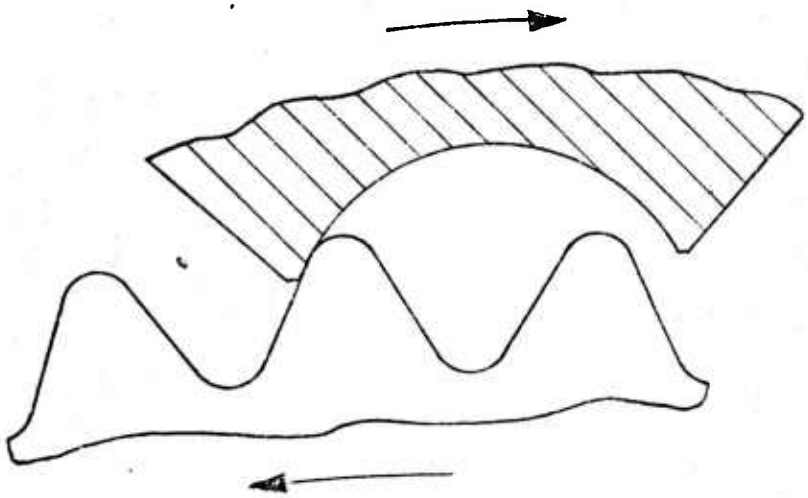

EXIT ENGAGEMENT

Figure 2. Engagement Contact

direction of setback will depress the pin far enough to disengage it from the rotor. If a spin level of approximately 2500 rpm is also present at this time, the setback pin will remain in the depressed position even when the axial force ceases. This setback system is utilized in the M125A1 Modular Booster and has proven to be a highly reliable system, even in mass production.

TECHNICAL CHARACTERISTICS OF THE FINALIZED PROTOTYPE DESIGN

The finalized prototype design has thus far proven to be a rugged device potentially capable of high reliability and widespread application in artillery fuzing. The following technical properties of the device have been noted and are listed below:

ARMING DELAY

The device in its present form (technical drawings are included in appendix) can be expected to provide approximately 24.5 ± 3 turns arming delay in spin environments ranging from 2000 to 20,000 rpm. Spin tests conducted as high as 30,000 rpm still yielded time delay on the order of 20 turns. Increased arming delay can be achieved with this device by modification of the pallet lever. The lever is shown in Figure 3 and can be seen to contain two .264 in. diameter lightening holes. Eliminating these holes would increase arming delay by approximately 10%. It should be noted that this action would not affect the unbalance torque on the lever since the c.g. of the lever would move toward the lever pivot exactly enough to offset the increased weight of the lever. This can be shown to be the case anytime weight is added symmetrically about the appropriate axis. The addition of this weight, however, can be predicted to increase both frictional torque and loading on the lever pivot. This may produce a corresponding decrease in both reliability at low rpm and strength at high rpm.

Another way to increase arming delay with this device is to reduce the diameter of the holes in the brass weights of the pallet lever. These weights are positioned .428 inches from the pivot position. Addition of weight here produces two effects which increase time delay. The inertia of the lever increases significantly even with the addition of a small amount of weight here because of the large radius of gyration associated with this position. The unbalance torque on the lever also increases when these holes in the brass weights are reduced in size since the increased weight of the overall assembly in this location shifts the c.g. further out from its pivot. Once again additional frictional torque would result possibly at the expense of arming capability at low rpm.

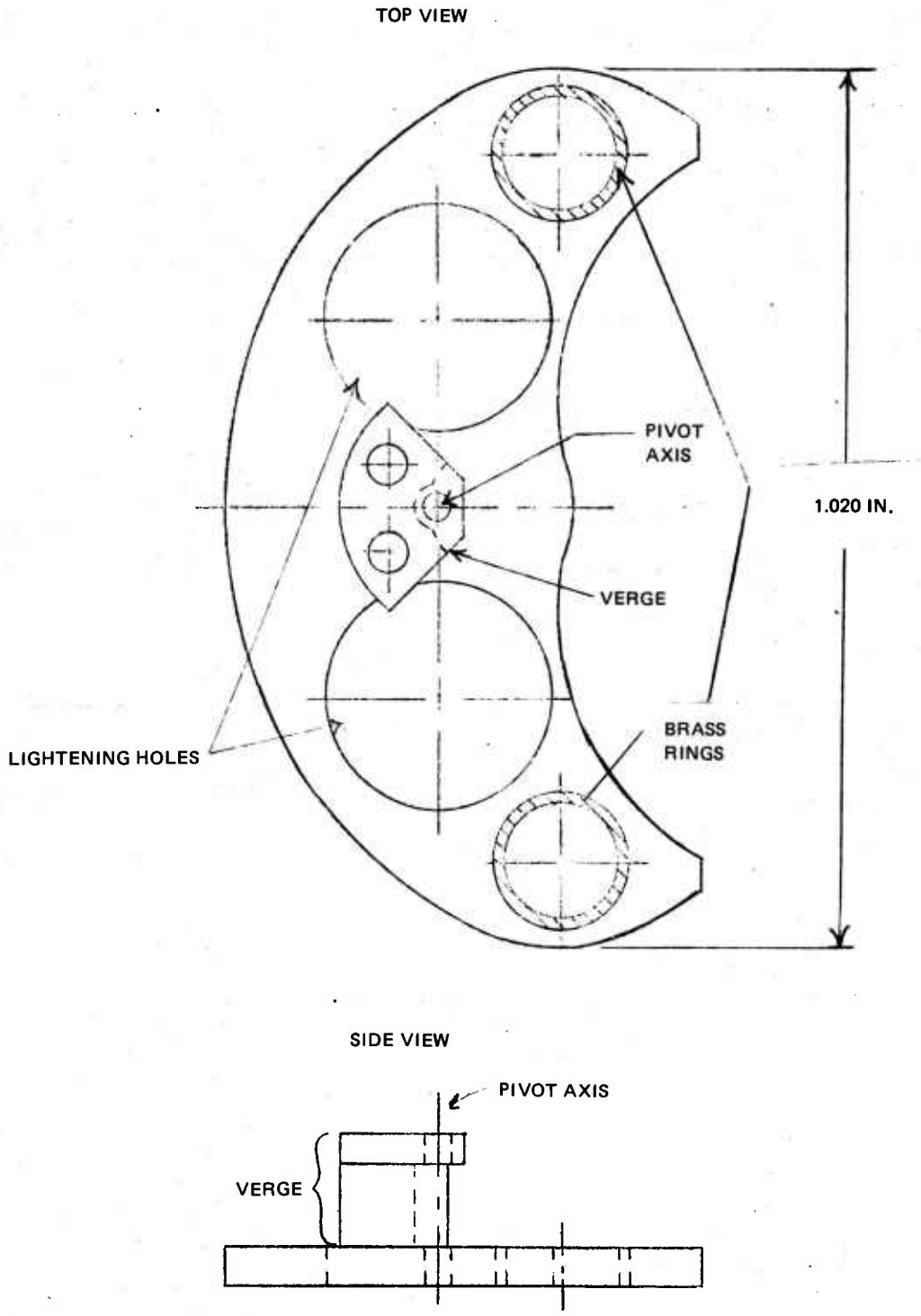

Figure 3. Pallet Lever Assembly

The best way in increase arming delay with this device is to increase the lever inertia without increasing its weight. This could be accomplished by redistributing the weight which already exists such as to be further from the lever pivot. This endeavor represents possibly the most fruitful area of future effort with this device. It is conceivable that a higher inertia lighterweight lever assembly could result, allowing further reduction in pivot diameter without sacrifice of strength. The overall reduction in frictional torque loss should be accompanied by increased reliability and performance at low spin levels.

Reduction in rotor torque will also increase time delay but caution should be exercised in this area.

ARMING CAPABILITY

The lowest spin environment encountered with present use artillery weapons is that of the 8 in. Howitzer (Model M110) at Z1 which yields 2950 rpm. Functioning rate in this environment with the final design was reported by TECOM to be above 95% (point estimate representing 1 dud in 24 rounds). The dud consisted of one unit found to have completed 85% of the timing portion of the arming cycle. Other ballistic testing conducted was in the form of arming distance tests from the 105 Howitzer at Zone 7 in which a standard deviation of 6.1 ft. was observed along with a mean of 168.6 ft. S&A devices driven by centrifugal force generally experience the majority of arming difficulty in low spin environments. High spin environments only present arming problems when structural damage is induced during interior ballistics which impedes the arming process.

Laboratory spin tests at low rpm indicate that the spin locks disengage at approximately 1500 rpm. The mechanism itself appears capable of operating at 1000 rpm.

LUBRICATION

This device is lubricated with a teflon dry film known as Slide-a-lon previously qualified for use in the M125A1 booster as reported in FA TR#R-20270. Coefficients of friction measured with this lubricant applied at full strength on a wide range of surface finishes with brass and steel indicate an average coefficient of friction of $\mu = .07$ and as high as $\mu = .22$. This lubricant can be diluted with trichlorethane-Nu and is applied by a simple dip process after which it air cures resulting in a coating thickness dependent on the ratio of slide-a-lon to solvent. Uncut it results in a coating as thick as .001 inches. Cut one part slide-a-lon to three parts solvent usually yields a coating approximately .0001 inches thick.

END ITEM COST

The projected cost of the original DVA design was $.50 per unit (1971 dollars) for large scale production. Configuration changes made since have substantially simplified the device and should result in a unit cost of $.68 per unit (1975 dollars) as compared with the cost of the M125A1 Booster Module of $1.25 per unit.

CHRONOLOGICAL REVIEW OF DESIGNS

The design in its finalized prototype version was preceded by several similar designs which indicated deficiencies or shortcomings necessitating configuration changes until a suitable device was achieved. In terms of operating torque characteristics there have been three designs. The rotor escapewheel assemblies in the second and third designs produced respectively 78% and 90% less torque than the first. The pallet lever inertia and weight were also suitably adjusted to complement their respective rotor torque outputs. Problems and shortcomings with these three basic designs are presented here briefly and are later amplified in detail.

The first design was bought from Delaware Valley Armaments, an M125A1 Booster contractor, together with 1000 models for Engineering Development Testing which eventually uncovered a condition wherein severe structural damage was taking place in high spin weapons (13,500 rpm and above).

The second design reduced the loading on the sensitive structural areas by 78% and resulted in both elimination of the structural wear and arming delay of approximately 28 turns in a 19,500 rpm spin environment. Low spin performance of this item (2000 - 3000 rpm range) was not satisfactory.

The third design utilized a rotor delivering only 10% of the torque of the original DVA rotor and contained four important configuration changes which increased low spin performance but reduced arming delay to 24.5 turns. Mechanism functioning in the 8 in. Howitzer at Z 1 (2950 rpm) - a problem low spin environment - was shown to be approximately 95% for a small sample (24 rounds). It is this final design which is recommended for future effort.

While there were three basic designs which fit the space envelope of the M739 fuze S&A, there were four slightly altered configurations of the third design. These alterations are described in detail later in this report. It should be noted that the "technical characteristics" of the device described previously pertained to Design III, Configuration 4 and is also referred to as the "finalized prototype version."

All ballistic test results are summarized in Table 1. A total of 235 rounds were fired overall. The following is a detailed description of all versions and configurations along with test results given on a chronological basis.

Table 1. Ballistic Test Result Summary

Design/Configuration	Weapon/Zone 7	Type Test	Remarks
Design I (DVA Design)	90 mm Gun M41	Board Non-Function	135 ft. -5/5 Function
Design I (DVA Design)	105 mm Gun M2A1	Board Non-Function	135 ft. -3/5 Function
Design I (DVA Design)	155 mm How.	Ground Impact	20 rounds tested; 1 dud
Design I (DVA Design)	90 mm Gun M41	Ground Impact/ Recovery	Structural damage in mechanism evident
Design I w/protective coatings	90 mm Gun M41	Ground Impact/ Recovery	Structural damage persists
Design II, Config. 1	90 mm Gun M41	Ground Impact/ Recovery	Structural damage eliminated
Design II, Config. 1	105 mm How. M103 Zone 7	Langlie Arm. Distance	Mean: 169.9ft --- 27.4 turns Std. Dev: 14.1 ft. --- 1.9 turns
Design II, Config. 1	90 mm Gun M41	Langlie Arm. Distance	Test suspended after 7 rounds due to erratic functioning
Design II, Config. 1	90 mm Gun M41	Recovery	Rotor shafts deformed
Design II, Config. 2	90 mm Gun M41	Langlie Arm. Distance	Mean: 83.8 ft --- 11.4 turns Std. Dev: 8.2 ft --- 1.1 turns
Design II, Config. 2	90 mm Gun M41	Recovery	No structural damage apparent
Design II, Config. 2	8 in How. Z1	Ground Impact SQ	10 rounds tested: 4 duds
Design II, Config. 3	90 mm Gun M41	Langlie Arm Distance	Mean: 210 ft --- 28.5 turns Std Dev: (too small to measure)
Design III, Config. 1	105 mm How. Z7 M103	Langlie Arm Distance	Mean: 129.0 ft --- 20.8 turns Std. Dev: 9.3 ft --- 1.5 turns

Table 1. Ballistic Test Result Summary (Cont'd)

Design/Configuration	Weapon/Zone 7	Type Test	Remarks
Design III, Config. 2	105 mm How Z7 M2A1	Langlie Arm Distance	Mean: 156.4 ft --- 23.2 turns Std. Dev: (too small to measure)
Design III, Config. 2	8 in. How Z1	Ground Impact SQ	22 rounds tested: 6 duds
Design III, Config. 2	155 mm How. Z1	Ground Impact Delay	10 rounds tested; 1 dud
Design III, Config. 3	8 in How. Z1	Ground Impact Recovery	20 rounds tested; 6 duds (with setback pins)
Design III, Config. 3	8 in How. Z1	Ground Impact Recovery	20 rounds tested; 1 duc (without setback pins)
Design III, Config. 3	8 in How. Z1	Ground Impact Recovery	(This group contained no setback pins) 4 rounds tested; 2 duds
Design III, Config. 3	8 in How. Z1	Ground Impact Recovery	10 rounds tested (with setback pins); 4 duds
Design III, Config. 3	8 in How. Z1	Ground Impact	3 rounds tested; 3 duds (torque sensitivity established before test)
Design III, Config. 4	105 mm How. Z7 M2A1	Langlie Arm Distance	Mean: 168.6 ft. --- 24.5 turns Std. Dev: 6.1 ft --- 9 turns
Design III, Config. 4	8 in How. Z1	Ground Impact	24 rounds tested; 1 dud

Basic DVA Concept

Figure 4 is a photo of DVA's demonstration model of a Gearless S&A. The device shown was the size of the M125A1 Booster module (larger than the present Gearless S&A) but contained the same basic elements. It contained no setback safety system but possessed a spin lock safety system biased with leaf springs similar to that of the M577 SSD. The rotor lock capability was provided by a leaf spring cantilevered from the rotor which was depressed toward the rotor pivot as the rotor armed. This spring would reopen when a particular rotor position was achieved such that a positive lock-out was secured.

The device in Figure 4 provided approximately 30 turns arming delay in a 2000 to 3000 rpm spin range which coincided with spin levels attainable with turns-to-arm measuring equipment available at the time. This model illustrated two important factors: first, that significant arming delay could be acquired mechanically through the use of two moving parts and no gear train; second, that the device still obeyed the turns-to-arm law. The ARMCOM search for a gearless device which would provide both these factors had previously produced little of any consequence. Ribbon delays, mass transfer devices, pyrotechnic delays, and cam follower mechanisms had been previously tried and found wanting in some respect (see Honeywell summary report of Contract DAAA-21-67-C-0866 dtd July 71). This Gearless device, however, was an evolutionary product of the M125A1 Booster module. It was still centrifugally driven and contained a runaway escapement, a combination which preserved the double integrating character of the mechanism. The high inertia unbalanced pallet lever, however, secured a low escapement oscillation rate producing the required arming delay. The "unbalance" effect of the pallet lever was strongly argued by DVA to be the key to the arming delay. Whether this is really the case is discussed later in this report in an analytical treatment of the "net lever torque". However, balanced pallet levers used in experiments still yielded appreciable time delay, but not as high as those with the unbalanced lever.

Design I Prototypes

Following a demonstration of this device in December 1969, DVA submitted an unsolicited proposal in June 1970 to design and fabricate a similar device to fit the M739 fuze (M572E2). This proposal was accepted and award of contract DAAA 25-71-C0229 took place in December 1970. This contract was to be conducted in two phases. The first phase was to consist of a design effort and submission of twelve prototypes made to this design. Following successful completion of this portion, the second phase was to consist of manufacture of one thousand S&A's for Engineering Development testing.

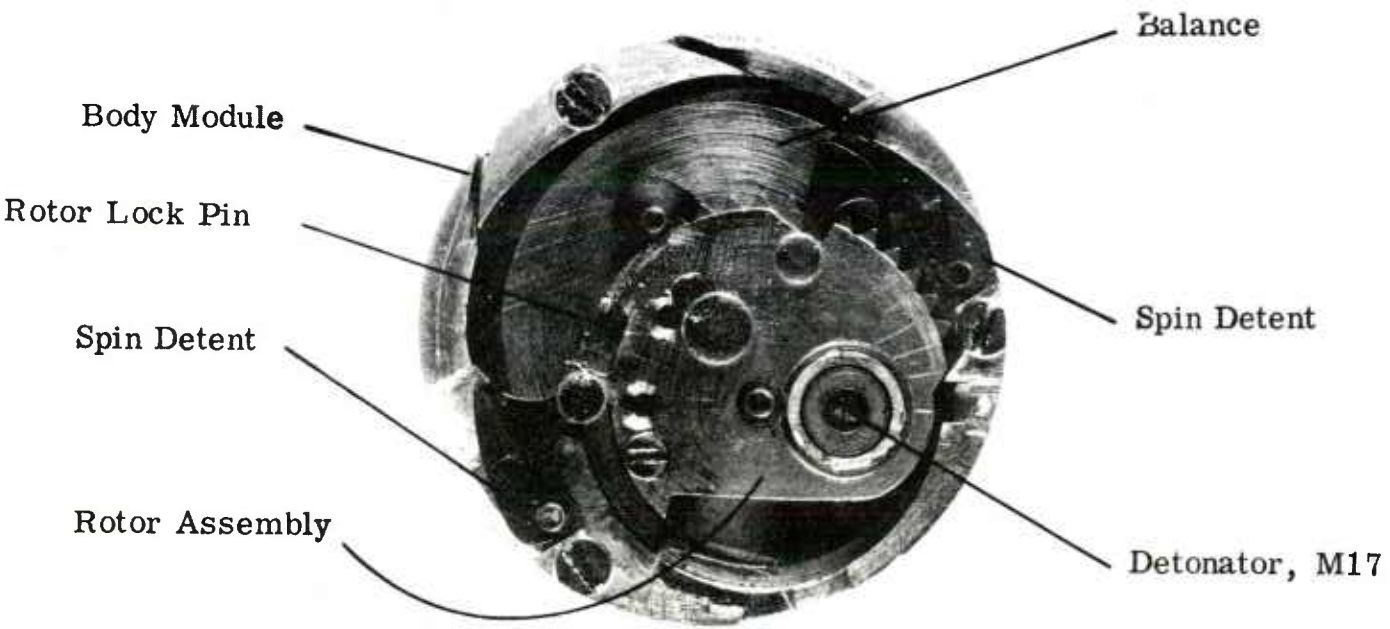

Figure 4. DVA Gearless Booster (M125A1 Size)

Phase 1 was eompleted seven months after award of contract. Four prototypes (see Figure 5) rather than twelve were submitted along with a set of engineering drawings to whieh the piece parts conformed dimensionally.

Testing performed on these four prototypes are summarized in Table 2. As no indieation of failure or potential failure was apparent, eight more prototypes were manufaetured for test. Indieation following test of all twelve prototypes were that this device met the basic requirements for an artillery S&A. Sinee all test results were satisfaetory, DVA was given authorization to continue with Phase II of the contraet involving the fabrietion of 1000 units.

Design I: Configuration 1

The Engineering Development test sample of 1000 units was delivered to Frankford in Mareh 72, fifteen months after award of contraet. Pre-ballistic testing results on this lot are summarized in Table 3. Ballistie Engineering Development Testing eommeneed in April 1972 at JPG but was suspended shortly thereafter owing to obvious premature arming of the S&A in high spin weapons. In the 90 mm Gun, Model M41, the first five eonsecutive units functioned on what was desired to be a non-function plywood target plaeed at 135 ft. from gun muzzle (approximately 13 turns).

Three of five units fired from the 105 mm Howitzer M2A1, Charge 7 (13,500 rpm), also functioned on 135 ft. targets. Recovery tests utilizing the 90 mm Gun subsequently indieated the presence of structural failure in the meehanism at two loeations: first, at the eseapewheel-verge eontact; secondly, at the lower pivot of the pallet lever. While in the second ease the lower pivots were only notieeably bent, in the first ease the verge faees and eseapewheel teeth exhibited shear failure involving the loss of approximately .050 in radius of the eseapewheel and .020 inches off the verge faees of the pallet lever assembly. The premature arming exhibited by this device was attributed to the wear and struetural damage apparent in this reeovery test.

Firings from the 155 mm Howitzer at Zone 1 resulted in one dud in 20 rounds fired. Recovery of this unit seemed to indieate a eondition wherein premature return of the setbaek pin stopped the rotor from arming. It was apparent that the rotor had moved from the fully safe position approximately four degrees.

A stress analysis was performed at this point by Dr. M. Jerry Koenig of Drexel University to quantitatively deseribe the amount by whieh the eseapement surfaces were being overstressed. Results of a theoretical investigation and

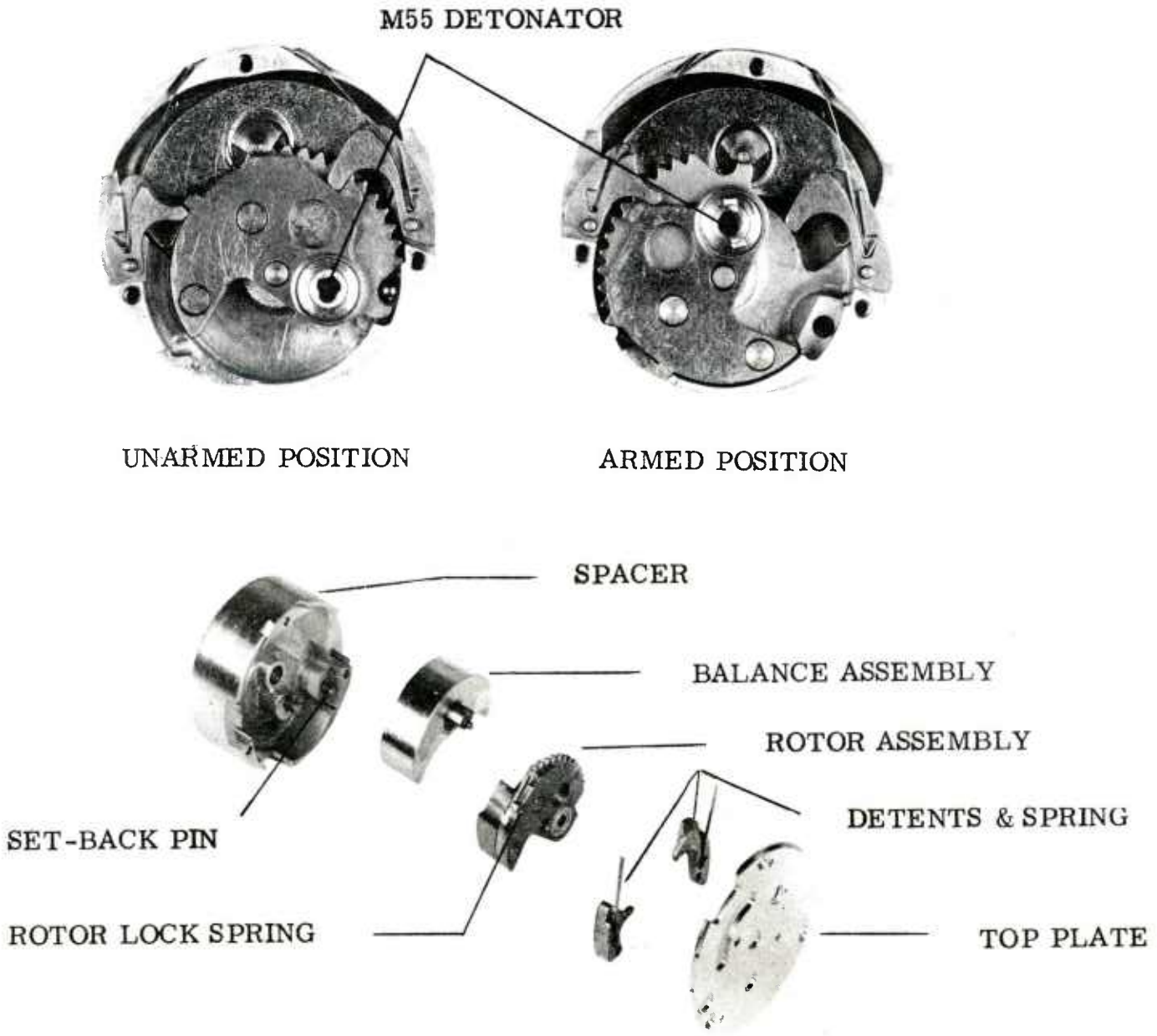

Figure 5. DVA Gearless Booster (M572E2 Size)

Table 2. TEST RESULTS SUMMARY - PROTOTYPES

TESTS CONDUCTED DURING DEVELOPMENT PHASE BY CONTRACTOR

ENVIRONMENTAL OR LABORATORY TEST	NUMBER OF UNITS SUBJECT TO TEST	RESULTS
Eccentric Spin Test	4	Armed up to .050 Eccentricity
Transportation-Vibration Test	2	Inspection revealed all locks engaged and Rotor Unarmed. Units were operational after test
Jolt Test	1	Inspection revealed all locks engaged and rotor unarmed. Units were operational after test
Jolt Test (Horizontal Position Only)	12	All units were tested for at least a two hour time period in horizontal position. Inspection revealed all locks engaged and rotor unarmed. Units were operational after test
Jumble Test	1	Inspection of unit revealed no damage. Unit was operational after test
Drop Test		
A. Five Foot	1	Unit Successfully passed test
B. Forty Foot	1	Unit Successfully passed test
Turns-to-Arm Test at 2000 RPM	4	Units were spun ten (10) times producing the following average turns-to-arm: #1 - 30.32 turns #3 - 34.92 turns #2 - 30.04 turns #4 - 30.86 turns
2000 RPM Spin Test	12	All units passed 2000 RPM arming Test

Table 2. TEST RESULTS SUMMARY - PROTOTYPES (Contd)

ENVIRONMENTAL OR LABORATORY TEST	NUMBER OF UNITS SUBJECT TO TEST	RESULTS
1000 RPM Spin Test	12	All units did not arm at 1000 RPM
Eccentric Spin Test	12	Units armed up to .0375" eccentricity
Air Gun Test (30,000 G's)	5	Inspection of units revealed no damage. Units armed three successive times at 2000 RPM after test.
Drop Test		
A. Five Foot	1	Inspection revealed all locks engaged and rotor unarmed after test. Unit was operational after test.
B. Forty Foot	1	Inspection revealed all locks engaged and rotor unarmed after test.
Transportation and Vibration Test	11	Inspection revealed all locks engaged and rotor unarmed. Units were operational after test.
Jumble Test	3	Inspection revealed all locks engaged and rotor unarmed. Units were operational after test.
Jolt Test	3	Inspection revealed all locks engaged and rotor unarmed. Two units were operational after test. The third unit failed the test when inspection revealed that the balance pivot had sheared off.

Table 2. TEST RESULTS SUMMARY - PROTOTYPES (Contd)

ENVIRONMENTAL OR LABORATORY TEST	NUMBER OF UNITS SUBJECT TO TEST	RESULTS
Jolt Test (Cont'd)		Unit was safe to handle but could lead to an unsafe condition in ballistics. The failure was traced to improper assembly of the balance assembly by DVA.
Static Detonator Test		
A. Phase I	8	Four (4) units were in unarmed position and four (4) in the half-armed position when the M24 detonator in the M48A3 Fuze was detonated. Inspection revealed that all eight(8) units had passed the test.
B. Phase II	8	The same eight (8) units were cleaned up and retested. This time holes were drilled in the top plate exposing the M55 detonators which were flash - detonated. Again four (4) units were in unarmed position and four (4) units were in half-armed position. Inspection revealed that all eight (8) units had passed the test.
Ballistic Test		
A. 105 mm Howitzer, Zone 7	4	Units were fired for recovery. Inspection of units showed that all units had armed and remained armed during impact. There was no damage to any of the components of the four models.

*Due to the limited number of models available, all the units were subjected to more that one environmental or ballistic test.

Table 3. ENGINEERING DEVELOPMENT TEST RESULTS

A. LABORATORY TESTS

1. 2000 rpm spin test - 997 out of the 1000 units armed. In the case of the three units, the cause of the failure to arm was the detents. However, the units did arm when subjected to a 2100 rpm spin test.

2. 1000 rpm non-arming test - all units did not arm as required.

3. Turns-to-Arm Test @3000 rpm - of the 1000 units

Mean	=	31.37 turns
σ	=	3.12 turns
$+3\sigma$	=	40.74 turns
-3σ	=	22.00 turns

4. Eccentric Spin Test conducted at DVA of 24 randomly picked units:

.040"	All armed
.060"	22/24 armed
.070"	0/24 - all did not function.

5. Inspection report - Twenty (20) units were inspected and all critical dimensions were within drawing tolerance.

6. Propogation test - All ten (10) units that were tested functioned as required.

B. ENVIRONMENTAL TESTS

A random sample of 10 units was subjected to each of the following tests:

Test	Result
Trans-Vibr	All units passed
Jumble	All units passed
Jolt	All units passed

Table 3. ENGINEERING DEVELOPMENT TEST RESULTS (Cont'd)

C. PRELIMINARY ED BALLISTIC TESTS

1. 155 mm Howitzer Zone 1 - Twenty (20) units fired for recovery, all but one functioned. The dud was caused by a set-back pin failing to function.

2. 90 mm Gun - service charge - At a spin level of 19,500 rpm in the 90 mm Gun, the first five consecutive units functioned prematurely on a 135 ft. plywood board (approximately 13 turns).

3. 105 mm Howitzer Zone 7 - Similarly, in the 105 mm Howitzer (13,800 rpm), three of the first five units fired functioned prematurely on a 135 ft. plywood board.

4. 90 mm Gun - service charge - Thirty (30) units were fired for recovery out of the 90 mm Gun. Examination of the recovered units revealed structural damage of the escapewheel teeth and verge faces.

analysis be performed are given in MR# M73-34-1 dtd November 73 entitled "Failure Analysis of a Gearless Safety and Arming Deviee." This analysis indieated that the failure mode was most probably one of dynamie bearing stress fatigue oecuring due to the impaet nature of escapement action. A eonservative estimate of rotor tooth impaet veloeity together with maximum rotor output torque indicated a life expectaney of the steel verge faces of 2 or 3 eyeles at 30,000 rpm and 4 or 5 cyeles at 17,000 rpm before plastic wiping away of the material took plaee. Since a full arming cyele consisted of 22 to 23 half eycles, premature arming due to dynamie overstress was a predietable oceurrenee. Recommendations made at this point were:

1. "To increase life by providing surfaees on upper balanee staff whieh are made of material whieh ean withstand high loads."

2. "Reducing the bearing pressures...by redueing the mass at the rotor and of the balanee."

Another possibility--inereasing the thiekness of the engagement surfaces (and henee inereasing the eross seetional area under stress) was not reeommended beeause of diffieulty in insuring full surfaee alignment. This suggestion was utilized later in prineiple by inereasing not the height of the eross seetion but rather its width aceomplishing the same end result. The first two reeommendations were adopted for main eourses of aetion to eliminate wear.

Design I With Proteetive Coatings

In aeeordanee with reeommendation **1,** various surface treatments and eoatings were applied to both the verge faees and the eseapewheel teeth to improve their load earrying ability. Table 4 lists the various eoating/treatment eonbinations tried and ballistie test results. None of these eombinations consistently yielded satisfactory results when subjeeted to actual test firings in the 90 mm M41 gun.

Design II; Configuration 1

The seeond course of aetion proved to be more successful. It involved redueing the torque output of the rotor along with a reduetion in weight and inertia of the pallet lever. This report later shows analytieally that this ean be accomplished without destroying the arming delay, low spin arming eapability, and double integrating character of the device. Prototypes implementing a 78% rotor torque reduetion and appropriate pallet lever inertia and weight reduetion were suecessfully fired from the 90 mm Gun, reeovered and indieated little struetural wear on all four units. This version, in addition to having parts lighter in weight, had a verge fabrieated from 7075T6 Aluminum to which was applied an electroless nickel coating. This coating was applied at a thickness of .001 inches using a small process outlined in Appendix 1 by the Corrosion

Table 4. 90 MM GUN BALLISTIC RECOVERY TESTS USING PROTECTIVE COATING ON VARIOUS COMPONENTS OF THE GEARLESS S&A

Escapewheel Coating	Verge Coating	Units Tested	No. of Units With Verges Damaged	No. of Units With Teeth Damaged	No. of Units w/No Damage
Electroless-Nickel	Electroless-Nickel	16	10	12	4
Hard-Coat Anodized	Electroless-Nickel	9	4	7	2
Electroless-Nickel	Electroless-Nickel plus coating of lead-tin solution	4	2	3	1
Hard-Coat Anodized	Electroless-Nickel plus coating of lead-tin solution	4	1	4	0
Hard-Coat Anodized	Chromium	4	4	3	0
None	Chromium	2	0	2	0
None	Electroless-Nickel	2	0	2	0

Research Division of Pittman-Dunn Laboratories. This coating, of itself, could not prevent the wear previously exhibited; but in conjunction with the reduction in bearing pressure proved successful. Nickel coatings had previously been used up until this time on the escapewheel assembly of the M125A1 Booster gear train for its friction reducing properties--escapement contact being a very friction sensitive area. The nickel's use here was for two purposes; first, to make the substrate aluminum more impact resistant; second, to prevent the poor bearing combination of aluminum on aluminum.

This device (designated Design II, Configuration 1) is illustrated in Figure 6. Aside from the lighter parts and reconfigured verge-pallet lever assembly, the rotor-escapewheel assembly now was designed to include an integral rotor shaft whereas the previous DVA design utilized a post pressed fit into the spacer as its pivot. A hole in the escapewheel fit over this post--similar to the arrangement used in the M125A1 Alt Booster. The L/D ratio in the case of the DVA Gearless mechanism was such that it permitted a tilt of the rotor assembly of .030 in. which could misalign the escapement verge faces and escapewheel teeth--reducing the effective bearing area supporting the escapement load. The inclusion of the shaft as an integral member of the rotor-escapewheel maintained the alignment to a higher degree. The possibility that this new shaft arrangement in itself might correct the wear problem was ballistically tested in the 90 mm Gun environment but was not successful.

Fabrication of hardware for Arming Distance Testing began early in 1973. Two Langlie "One-Shot-To-Failure" Tests were conducted from two high spin weapons, the 90 mm Gun (19,500 rpm) and the 105 mm Howitzer at Z7, M103 (15,7000 rpm). These tests demonstrated the first semblance of a "fix". In the 105 mm phase, a mean of 169.9 ft (27.4 Turns) and a standard deviation of 14.1 ft (1.9 turns) was indicated. However, in the 90 mm Gun phase, erratic functioning was observed and the test was terminated after seven rounds of firing. In summary, these two tests demonstrated that the mass reduction technique had extended the spin level survivability of the device to at least 15,7000 rpm. Recall that premature arming failures (19 turns) had been observed at 13,500 rpm with the DVA design. However, at 19,500 rpm some type of failure was still taking place.

Recovery tests fired from the 90 mm Gun indicated severe deformation of the rotor shaft whose inclusion in this design was previously discussed. This shaft was made of 2024T3 Aluminum.

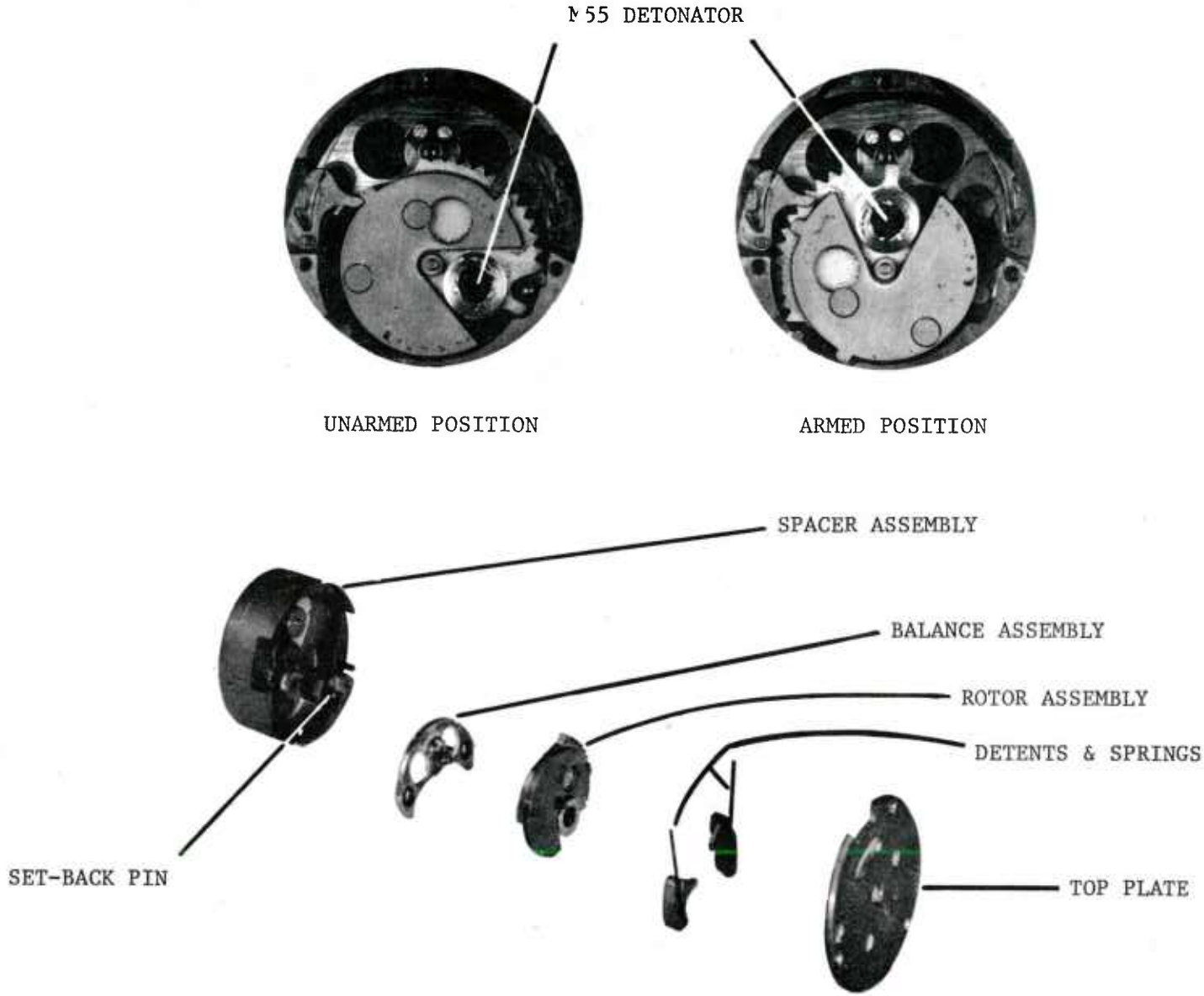

Figure 6. Gearless S & A – Design 2; Configuration 3

Design II, Configuration 2

The remainder of the test hardware was subsequently retrofit with stainless steel rotor shafts heat treated to a RC 38-42. An Arming distance test conducted at this time from the 90 mm Gun yielded a mean of 83.8 ft. (11.4 turns) and a standard deviation of 8.2 ft (1.1 turns). A Ground Impact Functioning test utilizing the 8 in Howitzer at Zone 1 resulted in four duds of ten rounds fired. The spin environment of this weapon-zone combination represents the lowest spin level to which an S&A on a spin stabilized projectile is subject and as such is a problem environment for all centrifugally driven spin actuated devices.

Included in this category is the returnable type setback pin used not only in the Gearless S&A, but in the M125A1 Booster (Figure 7), and M739 S&A. This setback pin can be depressed by an axial acceleration as low as 9 g's. In tandem with a spin level of approximately 2500, the pin will "freeze" against the sidewall of its cavity after its downstroke, releasing the rotor permitting it to advance out of the fully safe position. In the absence of this required spin level, the pin proceeds with its upstroke and resafes the rotor gear. This system was extensively tested during its development, and has since been incorporated into the M125A1 Booster and M564 and M565 Safety Adapters. As such, it has been even more extensively tested in lot acceptance testing and has proven to be a highly reliable device. Yet a similar design used in the M739 S&A (previous designation M572E2 S&A) caused a great deal of problems in low spin environments perhaps indicating the true complexity of what at first appears to be a simple friction damped spring mass system.

Aside from the indication of a low spin arming problem, the 11.4 turn arming delay in the 90 mm Gun environment was unsatisfactory. Even more puzzling was the fact that a recovery test fired shortly thereafter failed to indicate any structural damage in the mechanism other than the loss of approximately two thousandths of material from the verge faces--small in comparison to the extreme plastic flow noted before with the DVA heavyweight version and unlikely to be the cause of the serious deterioration in arming delay. Being a device of a double integrating nature, one would normally expect (in the absence of severe structural damage) the 27.4 turns arming delay exhibited at 15,700 rpm to be repeated at 19,500 rpm with perhaps a one or two turn variation due to the sensitivity of the test method. Instead the 27.4 turns deteriorated

1. James C. Mount, "Development of a Returnable Setback Safety Mechanism for Spin Activated Artillery", Frankford Arsenal Report R-1989, September 1970.

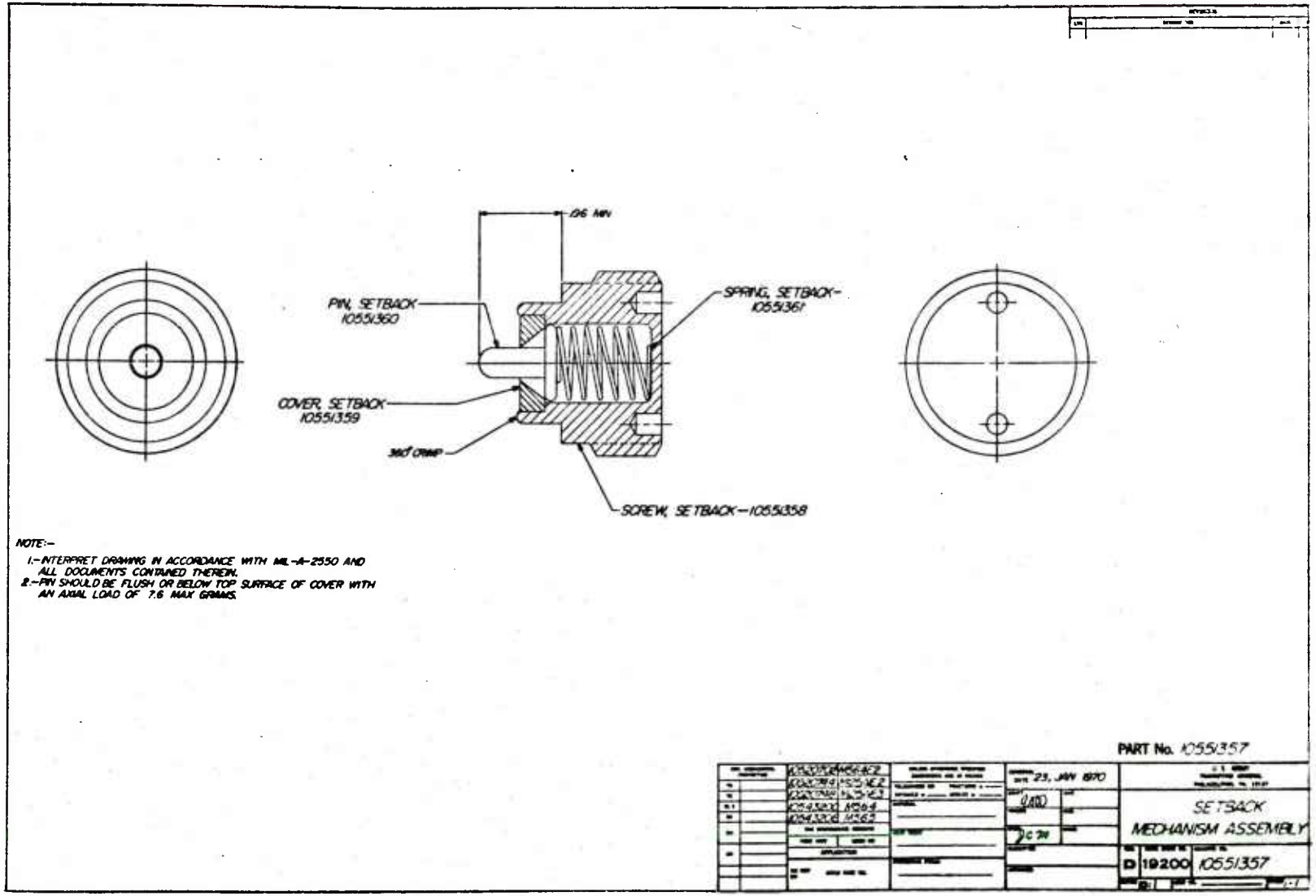

Figure 7. Returnable Setback System

into 11.5 turns with an increase in spin level of from 15,700 to 19,500 rpm. While this represents a 24% increase in spin velocity, it results in a 54% increase in centrifugal loading. It was therefore reasoned that a further reduction in rotor torque by $1-\frac{1}{1.54}$ or 35% should produce an acceptable device. It was here that the third design originated.

Design III, Configuration 1

Illustrated in figure 1, this design utilized a rotor assembly which generated 50% less torque than Design II providing a safety margin of 15% over that deemed necessary. In contrast with the original DVA design it generated 90% less torque and utilized a pallet lever 90% lighter in weight and was lower in Inertia by the same percentage. In addition the offset of the lever's c.g. from its pivot was maintained at .010 inches as in that of the original design.

It was subsequently discovered during laboratory testing of this design that this torque reduction was really unnecessary. A failure mode previously undetected was observed in a laboratory test at HDL on a high spin test rig. This piece of equipment has the capability of detenting the rotor until the desired spin level is achieved by the spinner motor at which time this detent can be released on command. An aborted test run in which this detent failed to release after the mechanism was brought up to 20,000 rpm indicated that the spin level alone, even before the escapement began to cycle, caused complete escapement disengagement. Further investigation was to show that this was caused by a tilting of a press fit support shaft under high spin. The manner in which this shaft supported the pallet lever is illustrated in figure 8, (upper illustration). Recall that this lever was much thinner than the DVA lever (.050 in. vs. .320 in) requiring a spacer of some sort to bring the thinner lever up to a height at which the verge faces align with the escapewheel teeth. This function was provided by a shaft press fit into the lower movement plate. This was to be a temporary arrangement as the thinner lever eventually would permit elimination of the lower movement plate and filling what was the lever cavity with die cast material forming a solid base. This backward tilt was eliminated by press fitting a support block between the spacer's cavity walls, and then securing this block to the lower movement plate using dowels and screws. This is illustrated in the lower portion of figure 8.

Design II; Configuration 3

Incorporation of this support block into the existing fuze hardware increased the arming delay in the 90 mm Gun environment from 11.5 turns to 28.5 turns (210 ft.) with a standard deviation too small to be measured with the Langlie Method using the "gates" utilized for this particular test.

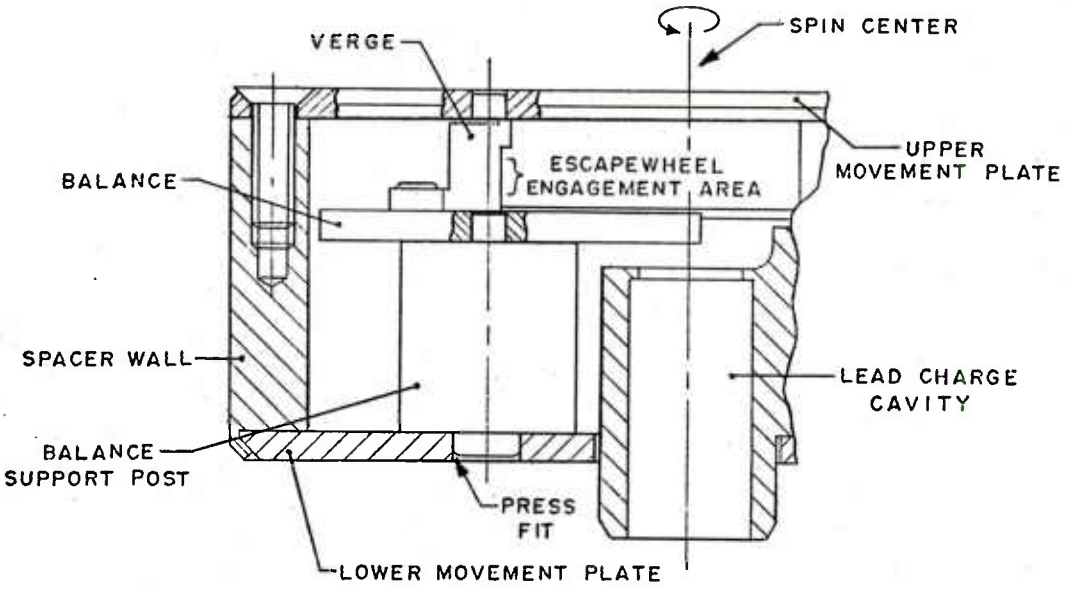

ORIGINAL PROTOTYPE DESIGN

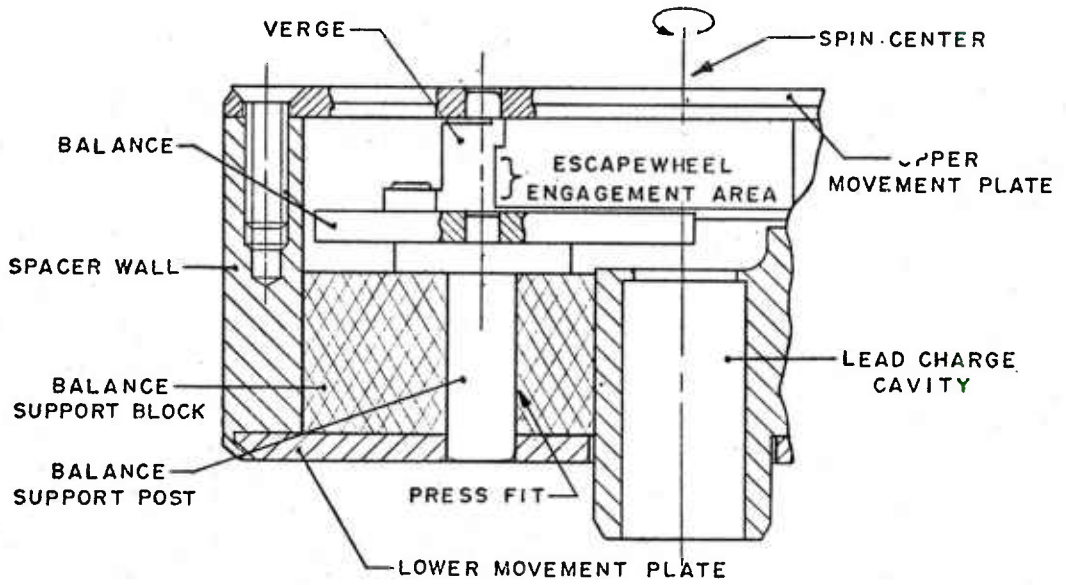

STRENGTHENED PROTOTYPE DESIGN

Figure 8. Lower Lever Pivot Configuration

These results rejected the hypothesis that the small amount of wear observed in recovery hardware was the cause of the arming delay deterioration. It also marked the first time that arming delay of any significant extent was demonstrated in a mechanical device without a gear train - in either a high or low spin environment. However, the fact that a 40% dud rate was previously experienced with this configuration indicated that further work needed to be performed on the design before continuing into a large engineering development test.

Design III; Configuration 1 (Continued)

Recall that a third design had already evolved at this point when the second design was still suspect insofar as structural integrity. One could logically conclude that knowing this second design to be sufficiently strong at 19,500 rpm, the third design which produced 50% less loading should be structurally adequate as high as 27,600 rpm. In addition the third design performed much better at low rpm in laboratory bench testing than did the previous design. A further advantage was that this design eliminated the top lamina of the rotor-escape-wheel assembly in favor of a cylindrical brass weight which served to locate the rotor's c.g. in it's proper orientation. The absence of the top lamina made possible the use of a ratchet-type pawl which swiveled atop the rotor to serve as a rotor lock feature. Illustrated in figure 9, the swiveling pawl contained a protruding pin which rode in a track cut into the movement plate. When the rotor disengaged the lever, the snap of the rotor into the armed position placed this pawl in a position such that centrifugal force flipped the pawl into a pocket locking the rotor in the armed position.

The advantage of this type system is that the frictional loss produced by this arrangement remains a fixed percentage of the rotor torque (estimated to be a loss of approximately 6%) regardless of the rotor's spin rate. This stands in contrast with the typical spring loaded pop-up pin used in the 125 Booster and 739 S&A which produces a fixed amount of frictional drag on the rotor causing a large loss in the mechanism at low rpm where rotor driving torque is at a minimum. The pop-up pin arrangement might also be desensitized by high spin via the same phenomenon that locks the returnable-type setback pin against the cavity sidewall.

The totality of advantages and potential capabilities of this third design led to a decision to pursue this version for future work. Three design changes made to this version prior to fabrication of additional hardware are described below:

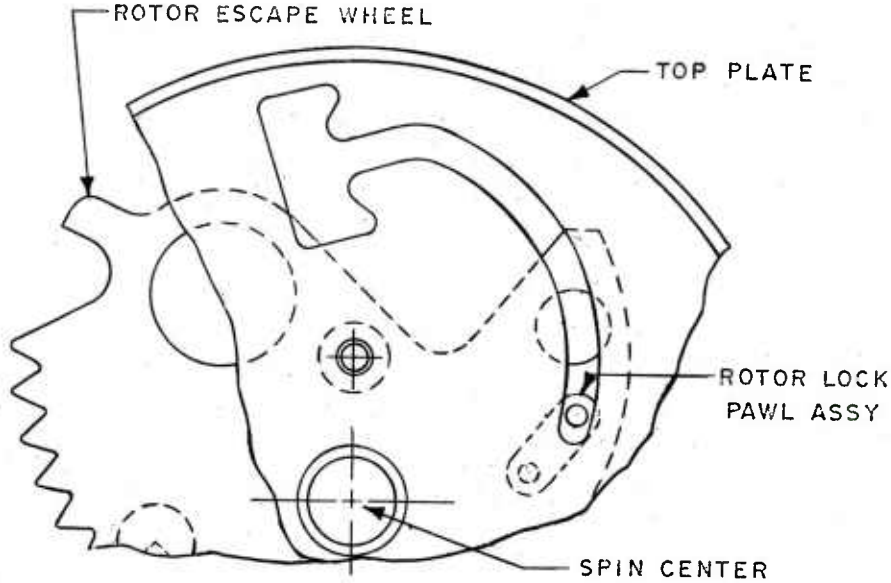

SAFE POSITION

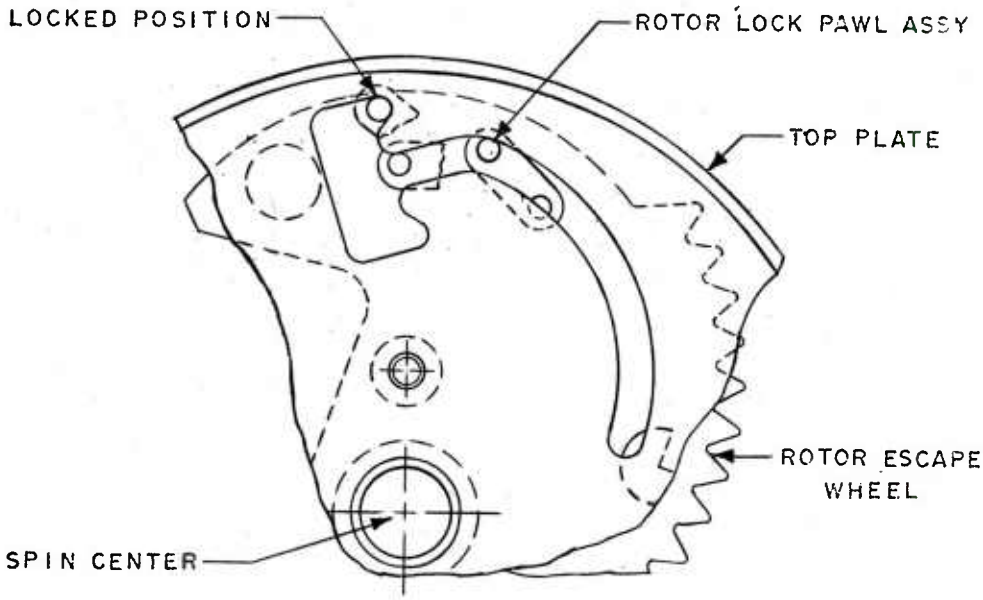

LOCKING SEQUENCE

Figure 9. Centrifugal Rotor Lock System

Lever pivot diameter reduction

Prior to this a .050 inch diameter pivot was being used for the lever. This corresponded to the original DVA design which contained a lever ten times as heavy. A reduction to .030 inch would predictably reduce the friction radius of the journal bearing in a very friction sensitive position - the lever pivot. This is illustrated in the second portion of this report.

Verge profile contour alteration

A CAD-E effort initiated to analyze shear cross sections of the verge faces, and to determine key escapement geometry parameters, identified several descrepancies and short-comings in the area of the escapement which could eventually result in difficulty. Utilization of the computer program and analysis developed indicated a verge face profile which corrected these noted shortcomings and produced a stronger verge face as well. This is illustrated in the following discussions:

Linkage Ratio and Efficiency.

Probably the most important two parameters one can know about a runaway escapement are its linkage ratio and efficiency. The counterparts of these two parameters for a gear mesh would be gear ratio and gear mesh efficiency. For an involute gear mesh properly designed the gear ratio remains constant. The mesh efficiency, however, constantly changes depending on the position of the contact points of the mesh relative to the line of centers. Clock gear meshes however yield changing gear ratios in addition to changing efficiency. The same is true of a runaway escapement mesh. For one, the gear ratio goes from plus to minus - this produces the oscillating motion of the lever as well as two distinctly different phases of motion which require seperate study - the entrance and exit phases of escapement motion. Secondly, within either of the two phases the linkage ratio (gear ratio counterpart) changes continuously yielding a set of values rather than a single value to be determined for each phase. Third, the friction sensitivity of the escapement mesh is distinctly different during each of the two phases and also changes within each phase.

The Linkage Ratio can be defined as $\frac{d\psi}{d\phi}$ where ψ is angular rotation of the lever and ϕ is angular rotation of the escapewheel. It can be determined graphically by taking the ratio of lines A_w and A_p depicted in figures 10 and 11 for entrance and exit engagement positions respectively. Lines A_w and A_p are the output and input force moment arms. The output force moment arm can be

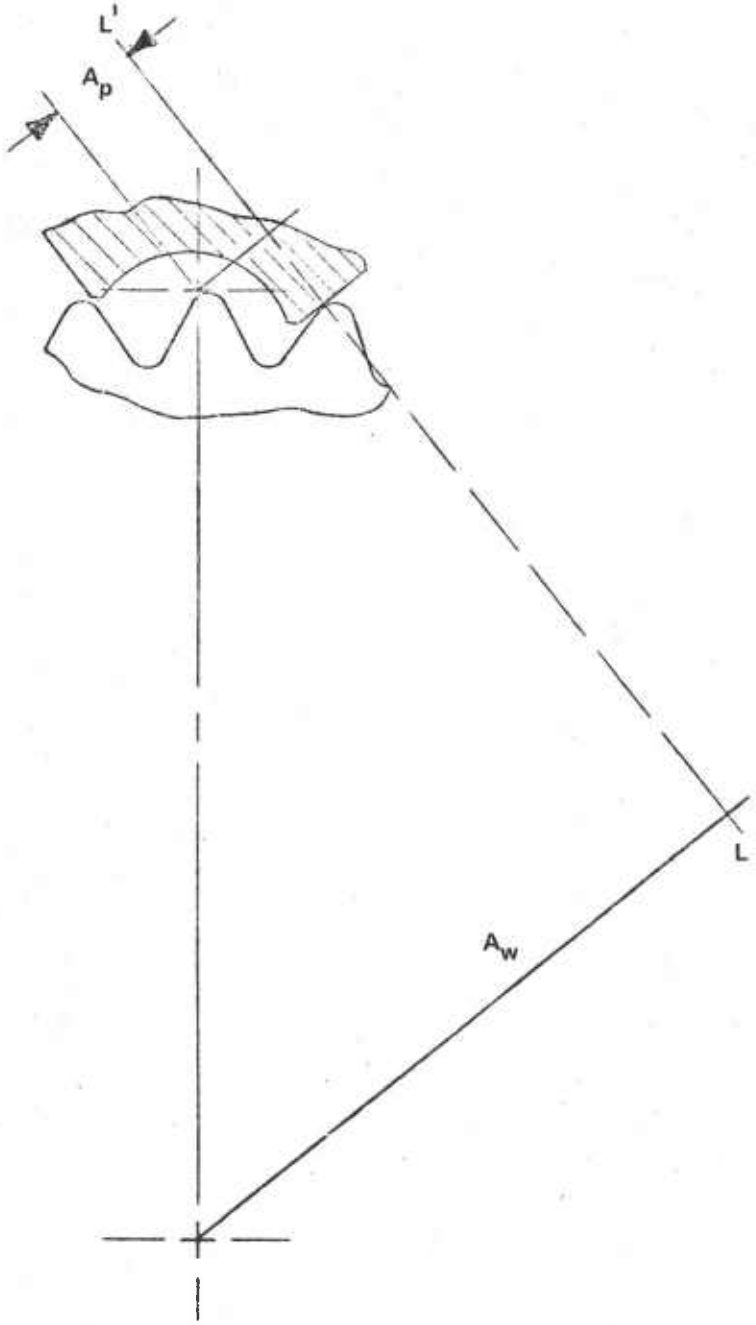

Figure 10. Escapement Moment Arms - Entrance Engagement

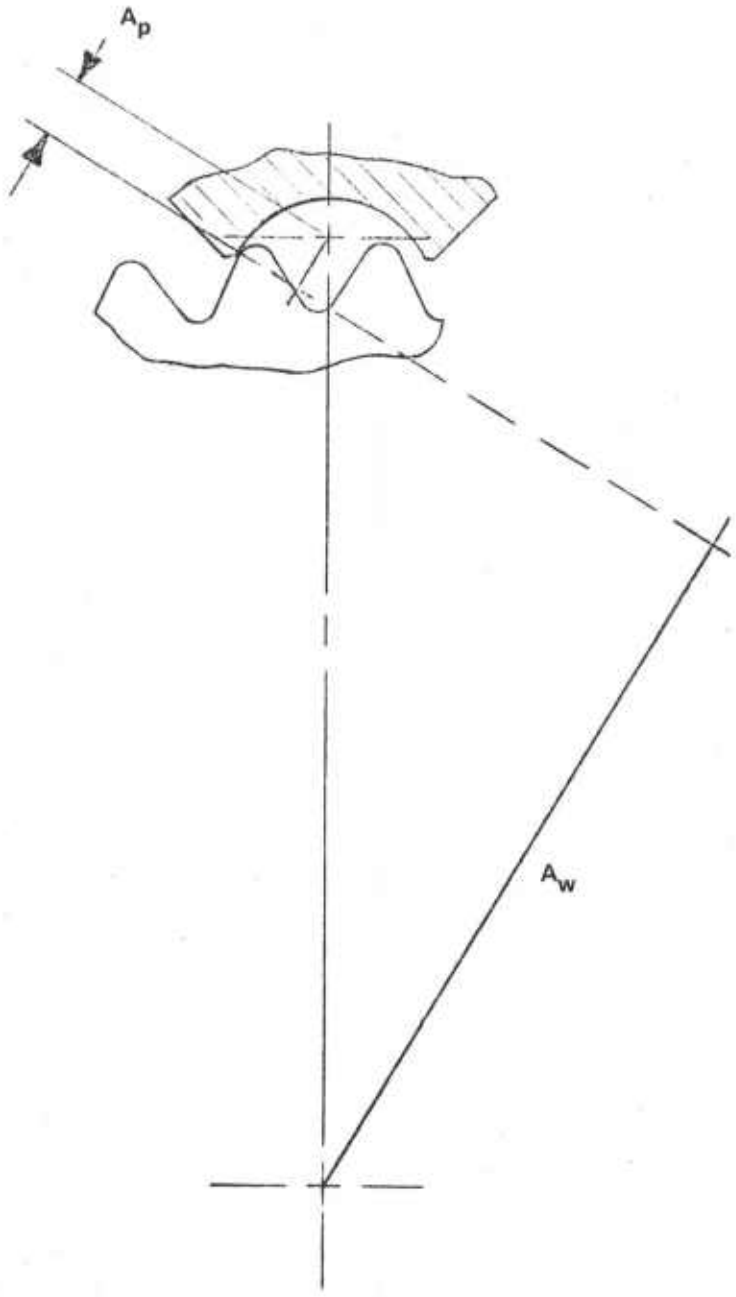

Figure 11. Escapement Moment Arms - Exit Engagement

used to estimate the magnitude of the force exerted on the verge face by the escapewheel. The linkage ratio can be used to determine the torque exerted on the pallet lever by the escapewheel. As such these parameters are very useful to know. The offset of the lever c. g. from its pivot makes knowledge of the linkage ratio even more important since the centrifugal bias changes as the lever rotates. The simultaneous occurrence of a high centrifugal bias and a low input torque (high linkage ratio) could result in a condition where no net torque acts on the lever which could cause it to stop motion (partially armed dud) or not begin motion if it has not yet started to move (fully unarmed dud).

In addition to other parameters to be discussed later, the computer program developed could determine the linkage ratio given a particular position of the pallet lever for either entrance or exit engagement. Figure 12 illustrates the values as they result for the original DVA escapement design. For entrance engagement the linkage ratio progressively increases and then tails off. This tail occurs due to contact between the tip of the verge and the tip of the escapewheel tooth as illustrated in figure 13. Contact prior to this occurs on the face of the verge rather than the tip. The linkage ratio is given as a function of lever position. The centrifugal bias numerically is proportional to the sin ψ such that the lever unbalance resists the escapewheel for $\psi<0$ and assists the escapewheel for $\psi>0$. With this in mind the shape of the linkage ratio curve prior to the tail is ideal realizing that high linkage ratio corresponds with low input torque. As the centrifugal bias decreases the linkage ratio increases. However, once the tail portion is reached the torques both from the escapewheel and from the unbalance are seen to simultaneously increase. In a sense this may appear to be a loss in potential time delay. However, it should be realized that this will serve to index the opposite verge face tooth deeper into the opposite space between the escapewheel teeth increasing the lever's angle of oscillation.

Analysis of the exit linkage ratio shape indicates that the input torque will be the lowest when the centrifugal bias is high - an undesireable condition. Comparison of the numerical values of entrance vs. exit indicates much higher linkage ratios, in general, on the exit side than on the entrance side. This would tend to produce an unbalanced beat - not undesireable in itself but less smooth and possibly more sensitive to stoppage. The changes made to the verge face profile contour served to make the entrance and exit linkage ratios more even. The linkage ratio on the exit phase was lowered and appears as in figure 14.

Linkage efficiency is a quantitative determination of what percentage of torque is transferred via a mesh in the presence of coulomb friction vs. what torque would be transferred were there no friction. For example, in a mesh

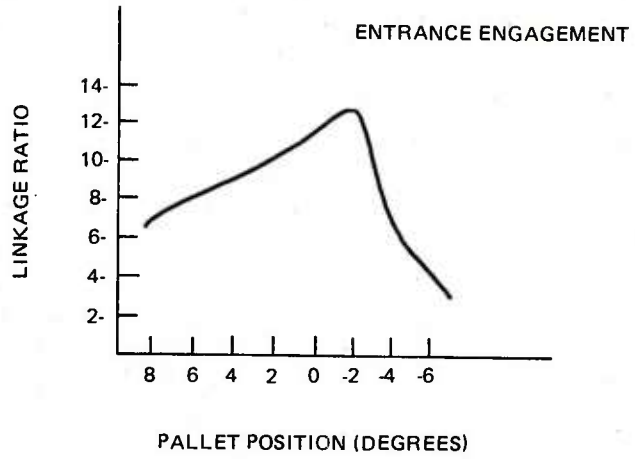

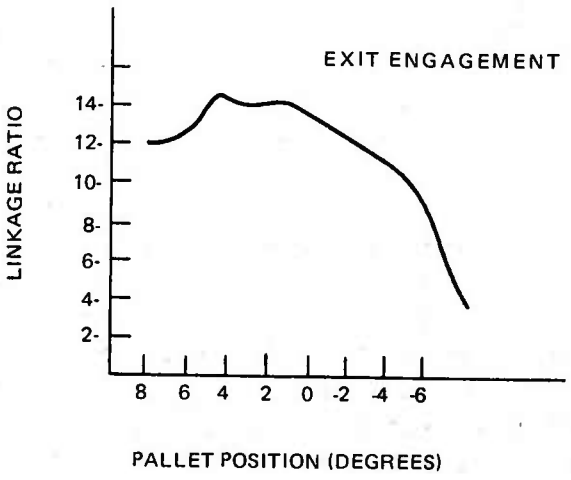

Figure 12. Linkage Ratio vs. Lever Position (DVA Design)

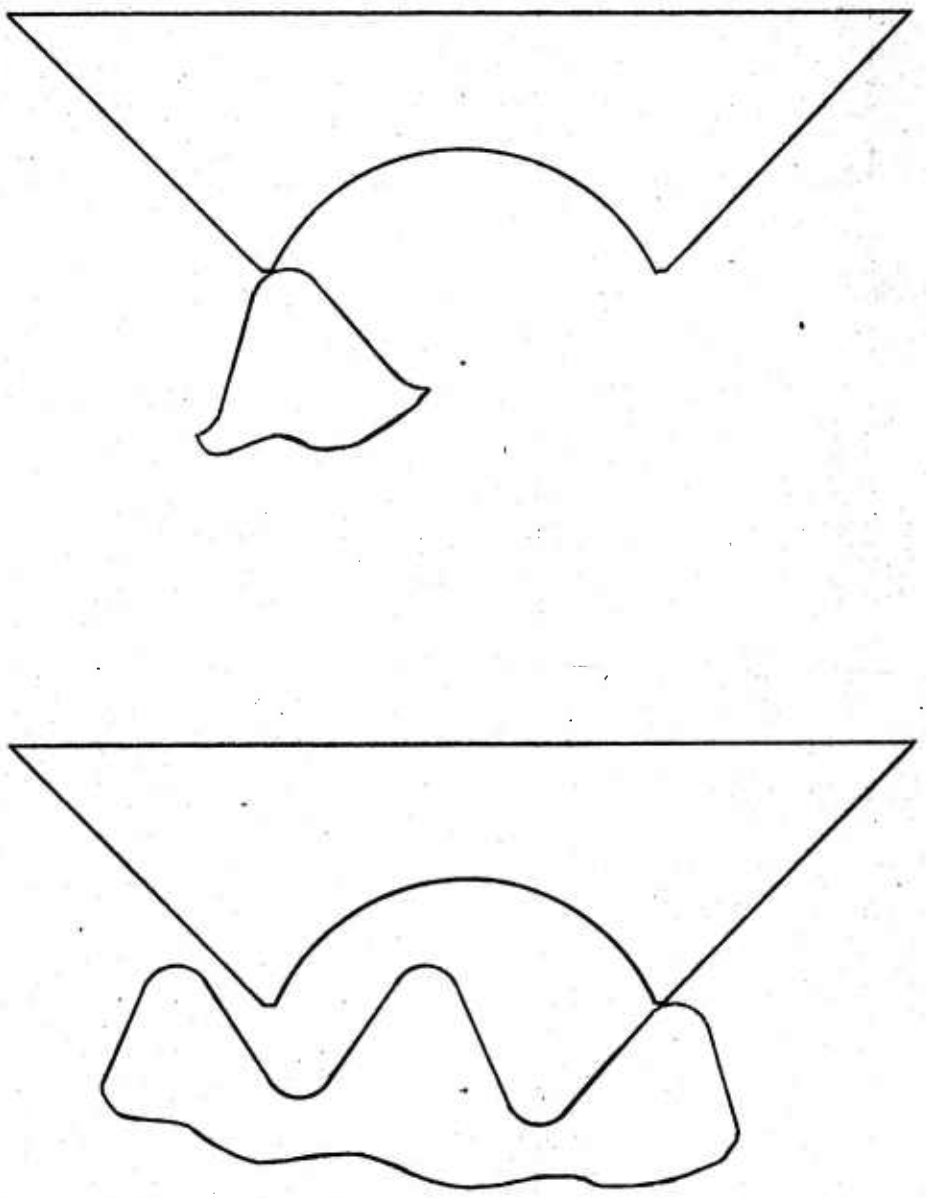

Figure 13. Tip Contact Positions

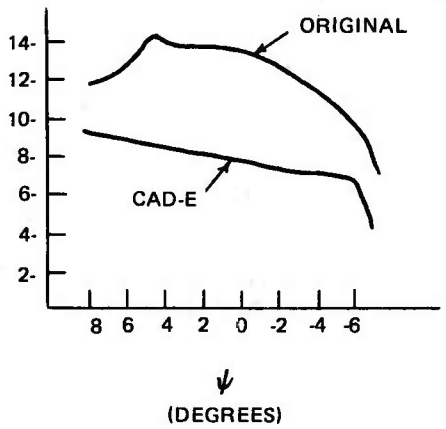

Figure 14. Exit Linkage Ratio - Original vs. CAD-E

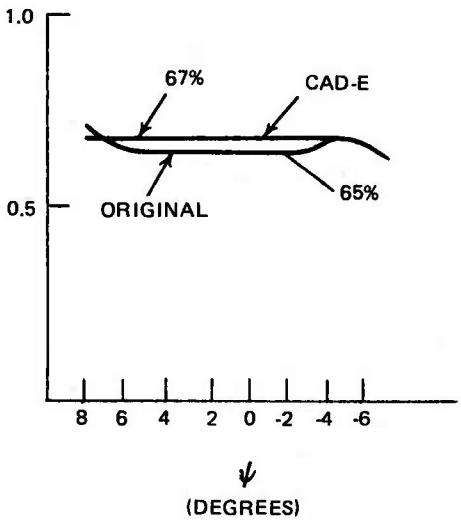

Figure 15. Exit Linkage Efficiency - Original vs. CAD-E

with a 10 to 1 gear or linkage ratio, an output torque of 10 in. lb from the gear would ideally result in an input of 1 in. lb torque on the pinion for the case of zero friction. If in fact only 1/2 in. lb torque was transmitted because the other half were lost due to sliding of the mesh surfaces over one another, that mesh could be classified as having an efficiency of 50%.

Efficiency in gears is strongly dependent on the pressure angle (generally 14-1/2 to 22 degrees), such that higher pressure angles produce lower efficiency. Runaway escapements, however, inherently operate at high pressure angles and are hence inefficient in comparison with gear meshes. It therefore becomes important to know the efficiency to be expected from an escapement mesh as well as the coefficient of friction to be expected. The Gearless S&A utilizes a verge or plate pallet runaway escapement whose "pressure angle" is dictated by the geometry of the verge face as opposed to pin pallet runaway escapements wherein the geometry of the starwheel predominantly dictates the pressure angle (factors such as center to center distance and escapewheel radius also affect efficiency and must be considered).

Analysis of the DVA-designed escapement indicated nothing alarming in terms of mesh efficiency in comparison with efficiency values previously calculated for the runaway escapement utilized in the M125A1 Booster. Figure 15 shows a graph of efficiency vs. lever position assuming a given coefficient of friction and contrasting the "improved" version with the original design.

Shear Cross Sectional Area.

The "W" shape of the verge faces produced dramatic differences in terms of wall thickness supporting the escapement load. Assuming this load is at all times "normal" to the verge face at the point of contact, it was found that loading at the tips was supported by a wall thickness of approx. .0007 inches. This was further compounded by the fact that the output moment arm of the escapewheel decreased as the contact approached the tip area. Assuming that

$$F_w = \frac{\text{Escapewheel Torque}}{A_w}$$

where F_w = output force of escapewheel

A_w = output moment arm of escapewheel

A strength parameter depicting load per unit wall thickness was devised, or

$$S = \frac{F_w}{Z}$$

i.e. $S = \frac{\text{Escapewheel Torque}}{(A_W) \qquad (Z)}$

where Z = wall thickness illustrated in figure 16 for entrance and exit contact.

The term $1/(A_W)$ (Z) is referred to here as a "shear stress coefficient" and is determined in the computer analysis. Figure 17 illustrates the curve of this parameter graphed vs. lever position. Separate types of loading were identified by geometry-moment arm interaction for each phase of engagement motion.

A. Entrance Engagement

Imposing the constraint that the direction of the applied force must be normal to both contacting surfaces (by definition of normal force), two types of contact result--face contact and tip contact.

1. Face contact

Figure 16 illustrates an escapewheel tooth in contact with the verge on the face position. Contact proceeds from point A to the tip at point B. It can be seen that a line normal to the verge face passes progressively through less and less material with the thinnest cross section occurring at the tip.

2. Tip contact

Figure 13 (top) illustrates this type contact. Since the tip is theoretically a sharp point, the direction of the line of action must always be normal to the radius at the tooth tip and as such rotates about the contact point so that the output moment arm shortens and the input moment arm lengthens as the rotor advances. This accounts for the deterioration of the linkage ratio. As this happens the line of action passes thru progressively thicker cross sections. However, the length of the output moment arm diminishes to zero. This theoretically leads to a condition wherein an infinite stress is applied to both contacting surfaces. In reality the inertia of the lever probably causes it to coast out of the way fast enough to avoid this action. This can be predicted to happen in every type escapement and even in gear meshes when the gear "runs out." The most severe gear tooth damage in an S&A is generally found on the last rotor tooth where it runs out. In that case the rotor is driving a gear stage massive in inertia compared to the rotor inertia. With the gearless S&A

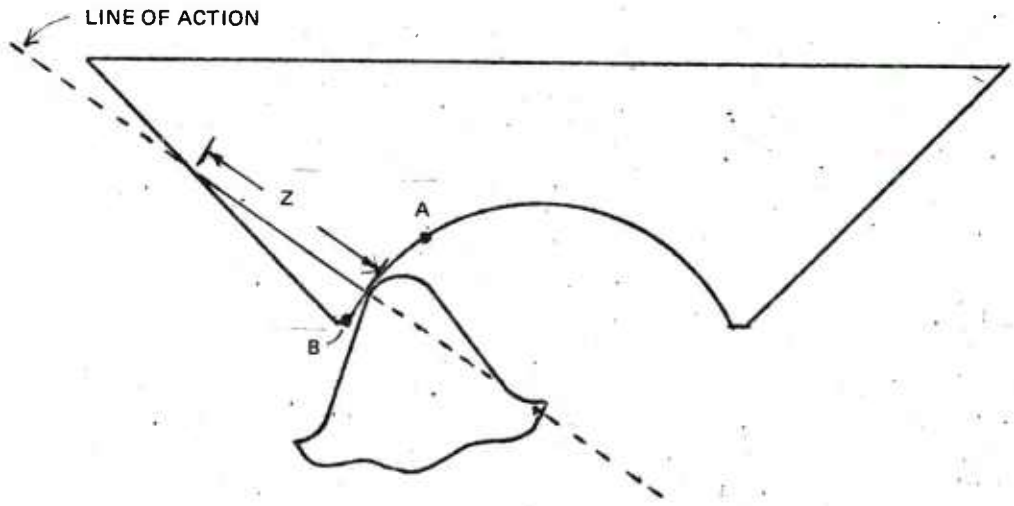

Figure 16. Top View - Cross Section Along Load Line

the rotor and escapewheel are approximately equal in inertia. The point at which the escapewheel and lever disengage must be determined by dynamic considerations and would be an ideal problem for computer graphics. The re-engagement point on the opposite tooth is similarly a dynamic problem and also important since it determines the true angle of oscillation of the lever which appears in the frequency equation.

The upper illustration in figure 17 shows the shape of this strength parameter for entrance engagement assuming a constant rotor torque. The large hump occurs during face contact and falls low as the line of action rotates toward the rotor pivot. The portion where this curve goes infinite has been cut off and was discussed above. The shape of this curve for the "improved" verge face contour is illustrated in figure 18 (top). The hump is eliminated by the stronger profile configuration. The shape of this "improved" contour is shown in figure 19.

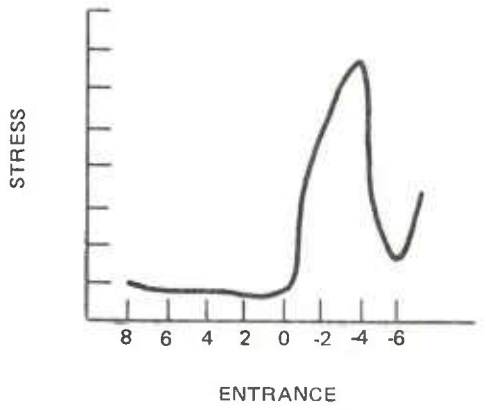

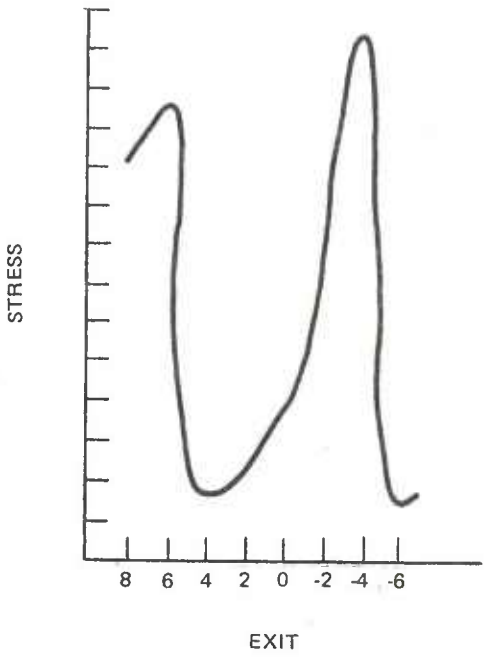

Figure 17. Loading Per Unit Length
vs.
Lever Position (DVA Design)

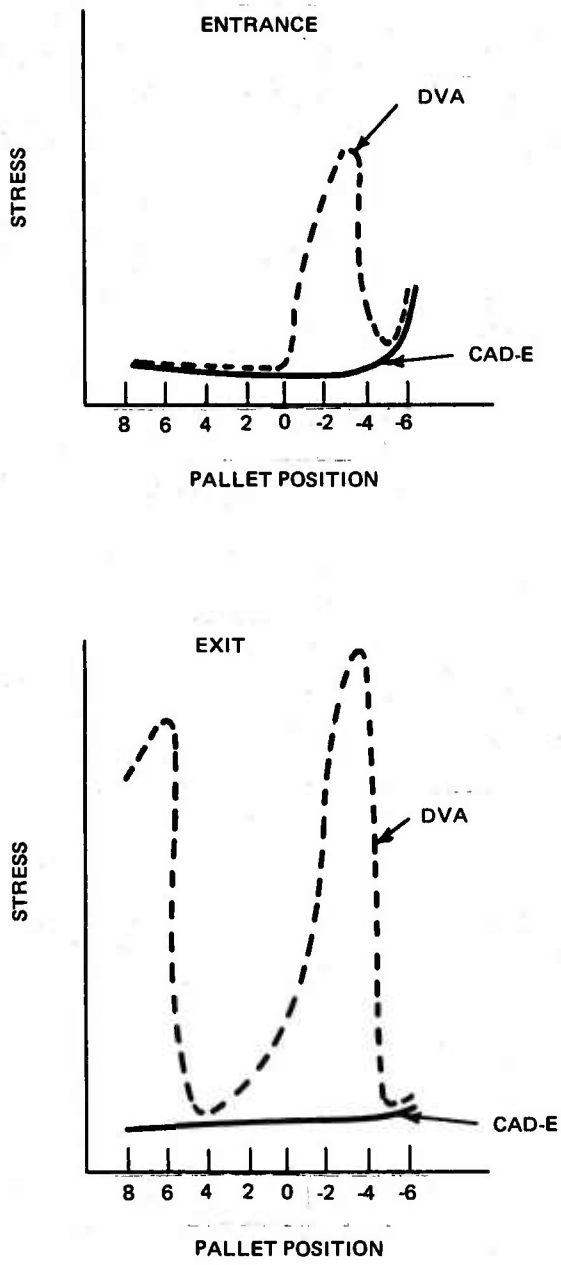

Figure 18. Loading Per Unit Length
(DVA vs. CAD-E)

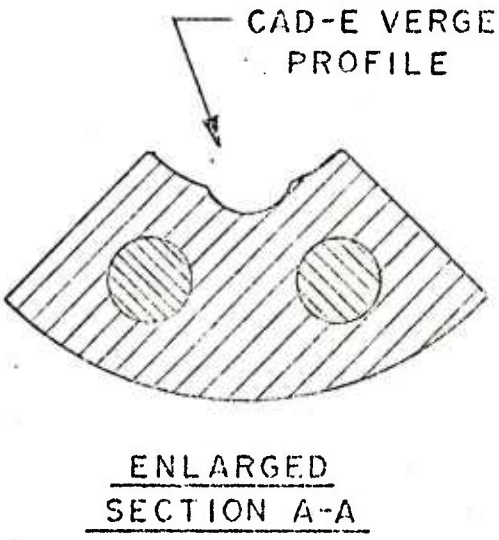

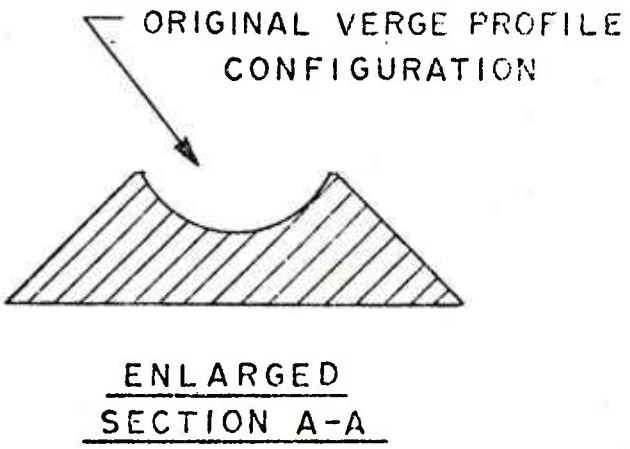

Figure 19. Verge Configuration Contrast

B. Exit Engagement

Three separate types of contact were exhibited by the original DVA design.

1. Verge Tip on Tooth Flank. This is illustrated in figure 20 and was found to be the only time where contact was ever made with the escapewheel tooth flank rather than the radius at the tip. This tip on tip contact takes place where the wheel and lever reengage which is of an impact nature likely to produce high "effective" loading in terms of damage or deflection it will produce. The lower illustration in figure 18 depicts the load per unit load line length for exit engagement. The high values at the left at the curve are caused by this tip on tip contact and do not assume any load magnification due to impact. This type contact was completely eliminated with the "improved" configuration.

2. Verge Radius on Escapewheel Tooth Tip. Illustrated in figure 16 this type contact proceeds from point A to point B and results in the line of action passing thru progressively thinner sections as contact approaches the tip. This accounts for the second hump in the curve.

3. Verge Tip on Wheel Tip. Illustrated in figure 13 (Top) this type contact is similar to tip contact on the entrance phase discussed previously. The line of action again rotates toward the rotor pivot producing an increase in load line length but a decrease in output moment arm length at the same time.

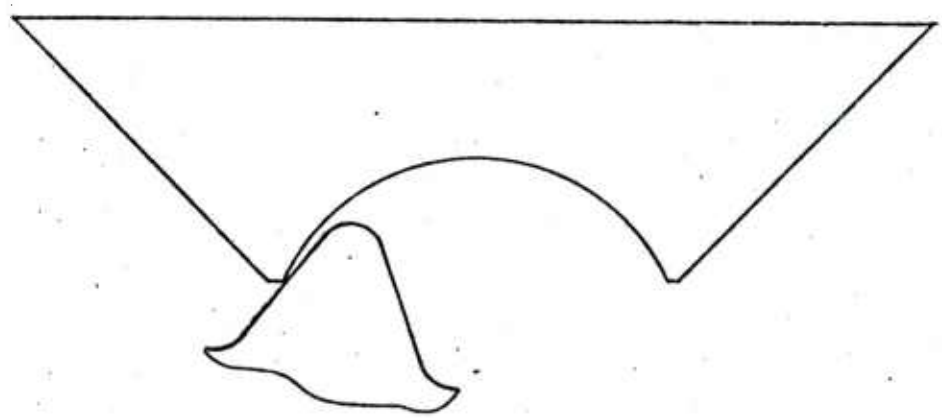

Figure 20. Verge Tip on Tooth Flank Position

Figure 18 illustrates the improved shear stress coefficient curve for exit engagement. It can be seen that the stress peaks have been eliminated producing once again a stronger profile.

Clearance. Escapement clearance can be defined here to be the smallest separation of the escapewheel tooth and verge on the side opposite that in engagement. Should both sides touch simultaneously the mechanism would jam. The trade-off made for the additional strength was in escapement clearance which was reduced to .005 min from a previous .010 min. There exist design changes to provide additional clearance should it become necessary.

Three Piece Verge Configuration.

The verge designed for the second design version was a single part riveted to the crescent shaped lever. It was found advantageous to split the verge into three pieces. One piece, the top pivot, was press fit into the upper movement plate and made to engage with a hole in the verge top rather than vice versa. A second piece, the verge hood, contained the hole with which to engage this pivot. The hood is required because the operational portion of the escapement is actually on the axis of rotation of the lever necessitating either a grossly undercut cylinder as a pivot or the assembly configuration utilized here. The third piece actually contained the verge surfaces used in escapement action. Figure 21 illustrates the multi-piece configuration vs. the one piece version previously utilized. This arrangement produced several assembly advantages. The first was that this configuration produced a more solid staking bed for the riveting tool. The previous verge tended to tilt backward while being riveted resulting in misalignment of upper and lower lever pivots. A second advantage was that a wire the size of the pivot could be passed thru the assembly maintaining pivot alignment during the riveting operation. Since one piece now became part of the movement plate, the verge portion of the lever now consisted of two pieces – a hood and base. This base portion is .100 in thick and can itself be laminated to accommodate a blanking process.

Five models incorporating these design changes were fabricated and exhibited substantially improved performance at low spin levels arming as low as 1000 rpm smoothly with no hesitation during the arming cycle: Turns-to-Arm tests at 3000 rpm indicated a mean delay of 27.5 turns which is tentatively acceptable. Additional hardware was fabricated for a ballistic arming distance test from the 105 mm Howitzer at Zone 7. The progressive twist weapon was used for this test to achieve a spin level of 15,700 rpm. The Langlie-One-Shot-To-Failure test sequence for fifteen rounds indicated a mean arming distance of 129 ft. (20.8 turns) with a standard deviation of 9.3 ft.

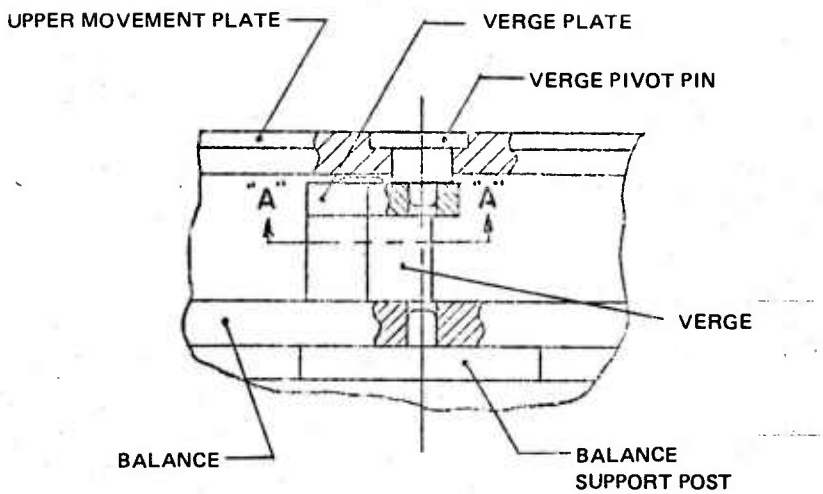

MULTI-PIECE VERGE

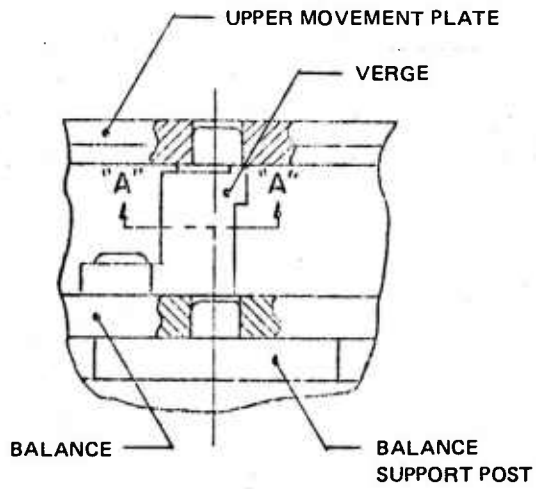

ONE PIECE VERGE

Figure 21. Single and Multi-Piece Verge Contrast

(1.5 turns). Comparison of laboratory arming delay with that exhibited in ballistic test on a unit by unit basis indicated a discrepancy as high at 7.8 turns indicating a poor correlation with ballistic testing.

Design III: Configuration 2

Investigation into the source of error uncovered a condition wherein a 15% loss in arming time was taking place due to the ability of the rotor detonator to set off the lead charge below it from a position wherein the rotor had not completed the last three half oscillations of arming. Inasmuch as twenty-three half oscillations make up the total cycle, these three represented a loss of as much as three turns. This was verified by a ballistic test from the 105 mm Howitzer at Z7 using a modified rotor gear in which the rotor detonator was positioned the equivalent of three half oscillations (12 degrees) further back in the arming cycle. This change, illustrated in Figure 22, resulted in a mean arming delay of 23.2 turns in ballistic testing representing approximately a 15% increase in arming delay. No standard deviation could be observed due either to the selection of the test levels for the Langlie or the tightness of the arming distribution. Since this arming delay was commensurate with that exhibited by the M739 S&A, no further design changes to increase arming delay were considered. Subsequent testing of this design with a solid die-cast spacer (Design III, Configuration 3) and without the make-shift spacer block/post arrangement indicated an even higher arming delay of 24.5 turns (mean).

Ground Impact Testing

Following demonstration of suitable arming delay, ground impact testing was conducted on 32 units yielding the following test results.

Weapon/Zone	Fuze Setting	Rds. Fired	Results
8 in. How. Z1	SQ	22	6 duds
155 mm How. Z1	D	10	1 dud

Investigation of the 8 in. Howitzer duds recovered showed the rotor moved out of the safe position to a point where it appeared to be stopped by the setback pin. Being a returnable pin it could not be ascertained whether the pin prematurely returned and blocked the path of the rotor or that the escapement jammed after running several oscillations after which the setback pin returned on ground impact. However, the consistent stoppage of the rotor in the area of the setback pin cast doubt on the performance of the setback safety system.

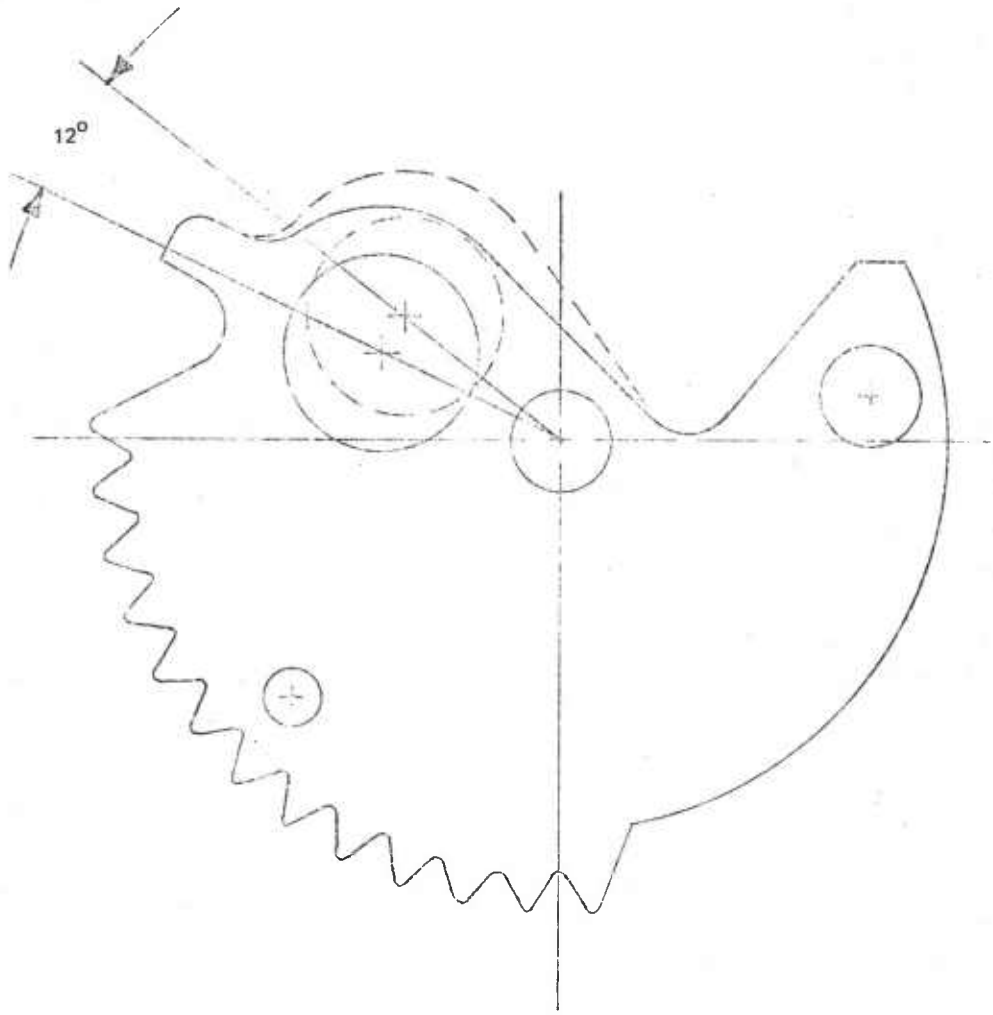

Figure 22. Detonator Shift

A test quantity was manufactured for ballistic testing with and without setback pins. Analysis of the setback pin insofar as its variance from the successful pin used in the M125A1 Modular Booster indicated the following:

1. Material difference. The M125A1 Modular Booster utilizes a brass setback pin. The Gearless S&A used the identical pin but made of stainless steel.

2. Distance from spin center. The setback pin cavity in the gearless S&A lies at a distance .528 inches from the spin center as opposed to .504 inches in the M125A1.

3. Spring Free Length. Both utilize identical setback pin springs; however, measurement of sample springs from Gearless S&A hardware indicated they were out of tolerance being undersize on the free length by several thousandths of an inch.

All other parameters of relevance were identical between the two designs. The above differences in combination appear to produce nearly equivalent systems insofar as the mechanics of setback pin response. Recall that this setback pin as used in the M125A1 Booster has been extensively tested and performs reliably in all applications. One would therefore expect similar reliable performance in the Gearless S&A application.

The following changes were made to the Gearless S&A design for purposes of correcting descrepancies associated with the setback system:

1. A brass setback pin as used in the M125A1 was utilized for future tests.

2. Whereas M125A1 Booster contractors were 100% load checking setback assemblies with a centrifuge, future setback pin and springs would be load tested in the same manner. This amounted to nothing more than obtaining small quantities of setback mechanism assemblies already qualified from a current M125A1 producer.

3. The arm extending from the rotor assembly whose purpose is to catch on the setback pin was made smaller in width (see Figure 23). This would eliminate failure in the case where this arm was positioned directly over a pin which prematurely returned after muzzle exit. Laboratory tests indicated the friction from this pin dragging on the underside of the rotor assembly was sufficient to prevent arming at 3000 rpm.

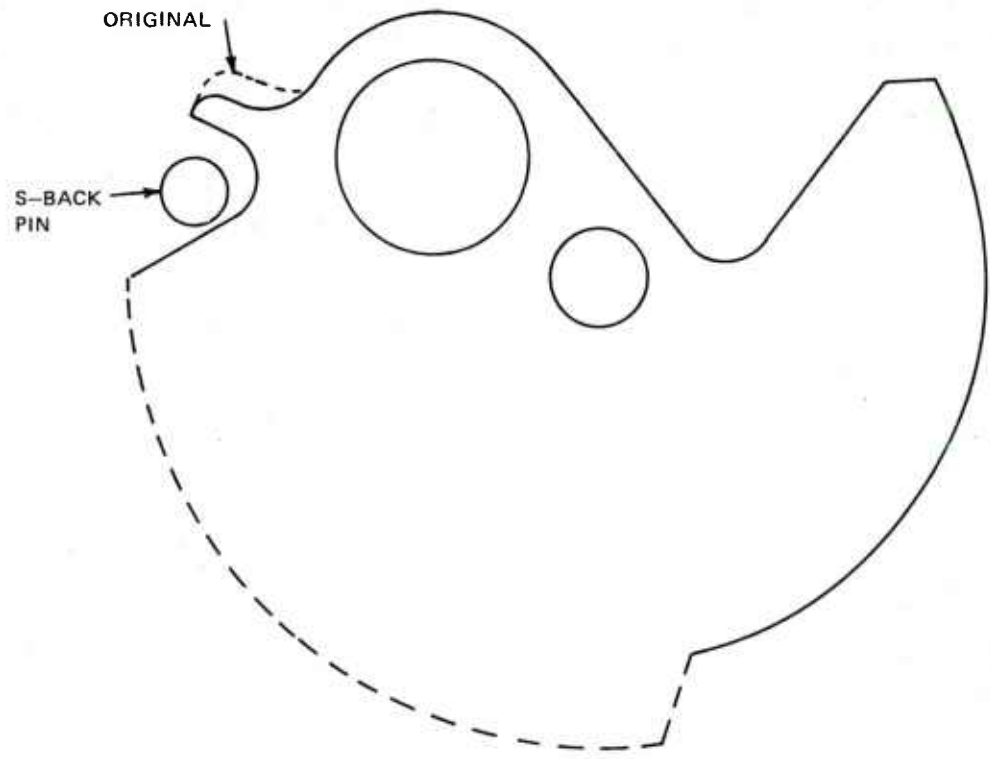

Figure 23. Setback/Rotor Interface – Original vs. Modified

A quantity was then fabricated for ballistic testing with and without setback pins.

Test Results

Group 1: This group contained brass setback pins. M55 detonators were loaded into the rotor gear assemblies at the Proving Ground. S&A's were then assembled and tested in load plant at 2000 rpm. All S&A's armed without hesitation. S&A's were then assembled into M572E2 fuzes with live M1 delay plungers and fired for recovery.

Weapon/Zone	Fuze Setting	Results
8 in. Howitzer/Z1	SQ	20 rounds recovered: 6 duds

Group II: This group contained no setback pins. Spin test following rotor loading and S&A assembly yielded four units which failed to arm initially but armed on a

respin at 2000 rpm. These four units were designated Group III. The remaining units which passed the test were designated Group II.

Weapon/Zone	Fuze Setting	Results
8 in. Howitzer/Z1	SQ	20 rounds recovered: 1 dud

Group III: This small group was the fallout from spin testing mentioned above. They contained no setback pins.

Weapon/Zone	Fuze Setting	Results
8 in. Howitzer/Z1	SQ	4 rounds recovered: 2 duds

FAILURE ANALYSIS

Dud Examination

Group I: These contained setback pins and passed a 2000 rpm spin test at the load plant prior to assembly into fuzes.

S&A #49: This unit was found approximately half armed and as such was definitely not a setback pin failure. The right hand spin lock spring was found wedged between the movement plate and the upper portion of the lever but it was not possible to ascertain whether this happened during flight or on ground impact since the blast of the M1 delay plunger severely damaged the guts of the mechanism. An imprint on the underside of the movement plate also shows this spring wedged in the lever's endshake indicating that if it was displaced on impact it did so shortly after impact before the powder imprint was made on the movement plate.

S&A #5: The rotor assembly was found advanced out of the fully unarmed position by approximately 4 degrees and against the setback pin. This may have been a setback pin failure.

S&A #8: The rotor assembly was found advanced out of the fully unarmed position by approximately 8 degrees such that the rotor's arm was over the setback pin. This may have been a setback pin failure.

S&A #22: The rotor assembly was found advanced out of the fully unarmed position by approximately four degrees with the arm of the rotor against the setback pin. This may have been a setback pin failure.

S&A #35: This unit was fully unarmed. The rotor did not move at all indicating an escapement failure.

S&A #19: This unit was fully unarmed. Powder burn marks on the underside of the movement plate show the right hand spin lock in the closed position. Whether this was the cause of failure could not be determined.

Group II: These did not contain setback pins and passed a 2000 rpm spin test at the load plant prior to assembly into fuzes.

S&A #27: The M1 delay plunger detonator initiated the M55 rotor detonator after impact and severely damaged the guts of the mechanism. It was possible to ascertain that the rotor was in the fully unarmed position when this happened.

Group III: These units contained no setback pins but initially failed a 2000 rpm arming test at the load plant prior to assembly into the fuze. They did arm on a respin however.

S&A #39: Same as #27. Fully unarmed.

S&A #44: The rotor assembly was found advanced out of the fully unarmed position by approx. 10°.

Comments:

Inspection of S&A #44 provided an important piece of information insofar as stoppage of the mechanism was noted after only one or two half cycles. Had there been a setback pin in this unit it would have returned on impact and appeared exactly the same as unit #8. This establishes the possibility that failures previously attributed to setback pins were really escapement failures.

Comparison of failure rates with and without setback pins indicated a contrast between 30% duds (6 out of 20) vs. 12-1/2% duds (3 out of 24) which at first glance appears significant. However, if use is made of observations made on recovered hardware, little contrast is evident. S&A #49 was partially armed - clearly not a setback failure. S&A's #35 and 19 were fully unarmed with the rotor four degrees away from a position wherein the setback pin could have interfered with arming. Counting these three as escapement failures the contrast becomes 17.6% (3 duds out of 17) with setback pins and 22.2% (6 duds out of 27) without setback pins. While this does not rule out the valid possibility that some duds were caused by setback pins, it does appear to indicate that some failures were being caused by escapement stoppage. Disadvantages of small

sample testing here are obvious but unavoidable when testing with expensive hand made prototypes. However, the ability to recover hardware after firing does at times provide a great deal of insight into the cause of failure when it does occur.

Torque Sensitivity Investigations

The M125A1 Alt Booster was at one time identified as being sensitive to an excess assembly torque when assembled onto the M48A3 fuze. The tightening of the booster bottoms the fuze on the upper movement plate of the booster mechanism and apparently depresses it to some small degree diminishing endshake and at times causing failure to arm. The gearless S&A is sandwiched between the delay plunger retainer and the S&A retainer. Spin testing using a fuze sleeve from an M572E2 fuze indicated a definite torque sensitivity of three of thirteen gearless S&A's from the same lot as the ballistic sample. The application of 50 in. lb assembly torque was found capable of eliminating lever endshake and jamming the mechanism with these particular units. This sensitivity was found to be caused by a misalignment of upper and lower lever pivots in the spacer and movement plate. This caused the lever to sit in a slightly cocked position on its bearing pad.

Eccentric Spin Tests

The possibility that eccentric spin of the projectile might cause S&A failure was explored. An eccentric spin fixture capable of producing eccentric axis rotation in increments of .015 inches was used. (See Table 5)

S&A's were tested in eight equally spaced orientations for a given eccentricity until a position was found wherein the rotor would either not begin to arm or not arm sufficiently to show the M55 under the flash hole. At that point a lower eccentric spin position was tried once more for eight orientations, etc.

Ballistic Tests

A ballistic test was conducted using these S&A's with the exception of units 71 and 57 which appeared more sensitive to eccentric spin. All ten units contained brass setback pins. Inert delay plungers were utilized to assure any movement plate powder burns took place on Ground Impact. All units were prequalified with 25 in. lb at 2000 rpm. This same assembly torque was utilized when the S&A's were assembled into fuzes at the Proving Ground. Results are as follows:

Table 5. Results of Eccentric Spin Tests

S&A	Radial Eccentric Spin Capability (RESC)
29	.045<RESC<.060
23	.045<RESC<.060
59	.030<RESC<.045
61	.045<RESC<.060
2	.015<RESC<.030
10	.030<RESC<.045
71	0 < RESC<.015
57	0 < RESC<.015
13	.015<RESC<.030
75	.015<RESC<.030
18	.030<RESC<.045
25	.030<RESC<.045

Weapon/Zone	Results
8 in. How. Z1	10 rds. fired: 4 duds

The three torque sensitive S&A's identified previously were also fired and resulted in duds as expected. These were assembled into fuzes with 50 in. lb assembly torque.

Recovered Dud Evaluation

No correlation between eccentric spin sensitivity and S&A malfunctioning was evident. Of the four duds, two were from the .030<R<.045 group, one from the .015<R<.030 group, and one from the .045<R<.060 group.

S&A #2: The rotor in this S&A was found to be in the fully unarmed position. Proper functioning of the left hand spin lock was questionable with the powder burn imprint indicating the spin lock closed on impact.

S&A #10: Rotor in fully unarmed position.

S&A #18: Rotor advanced from fully unarmed position approximately 4 degrees such that arm of rotor was up against setback pin. This may have been a setback pin failure.

S&A #61: Same as S&A #2.

Spin Lock Investigation:

While it was not certain that any failures were caused by spin lock malfunction, the powder burn imprint on two of the recovered duds did not clearly indicate the left hand spin lock to be positively open on impact as can often be easily ascertained. Inasmuchas the angular deacceleration of the projectile tends to make all rotating parts turn counterclockwise within the mechanism during target penetration, one would expect the left hand spin lock to open on impact. The opposite is true of the right hand spinlock; it tends to close. This opening and closing action applies to all parts able to rotate whether they be balanced or not. However, if they are unbalanced (as the spin locks are), an additional moment is created depending on the orientation of the spin lock c.g. with respect to its pivot at that particular instant. In addition, for non-normal or graze impact an additional force acts on all centers of gravity in the mechanism generating moments on those parts being unbalanced. One can readily see that motion of rotary members during the terminal ballistic environment is very complex making it difficult to ascertain with any certainty the position of the parts before impact by observing their position after impact.

A review of the spin lock design indicated several areas of possible improvement especially insofar as the left hand spin lock was concerned. A unique mode of failure was found to exist with the spin lock safety system in this device. Unlike other S&A's, the gearless S&A utilizes its spin locks in series rather than in parallel. In the fully safe position, the right hand spin lock secures the rotor. The left hand spin lock does not come into play until the right spin lock is defeated. In contrast, other S&A's have both spin locks simultaneously securing the rotor. One might predict that the Gearless S&A would henceforth be less safe because of this were it not for the fact that the force which would defeat the left hand spin lock would necessarily be in an orientation such that it drives the pallet lever clockwise. However, for the rotor to "escape" while the spin lock is temporarily disengaged, the rotor must turn the lever counterclockwise. The same is true of the right hand spin lock. The force which would defeat the spin lock would be of such an orientation so as to lock the lever preventing the rotor from escaping. This seems to make the spin lock safety system's effectiveness dependent on the presence of the pallet lever. In fact, this may well be true of all current S&A's in the sense that the

gear train in itself extremely lengthens the response time of the rotor gear. Remember that to completely defeat a spin lock, the rotor must move toward the armed position by a given amount before the spin lock returns to secure it. For a given forcing function, the time the rotor takes to move far enough to avoid subsequent recapture depends on its "effective inertia" which is possibly two orders of magnitude higher than its polar moment of inertia if a gear train and escapement are linked to the rotor. Similarly this would be the case with the Gearless S&A in which the rotor is linked to the pallet lever. Testing S&A's with the gear train deleted would give the best indication of how much the effectiveness of the spin lock safety system depends on the members linked to the rotor.

Problems with the spin lock safety system in the M125A1 Modular Booster centered about the friction lock at times created at the point where the rotor comes in contact with the spin lock. It was observed that the spin lock would work properly if it did not contact the rotor. However, it would friction lock if the rotor were in contact. This was subsequently remedied by changing the geometry of the rotor in the contact area such that the moment arm of the frictional force creating the lock was reduced. The fact that the left hand spin lock in the Gearless S&A does not fully engage the rotor in the unarmed position could conceivably produce a situation wherein the spin lock appears to work fine in pre-ballistic spin tests but jams when the spin lock opening sequence is reversed. Should the angular acceleration at launch open the right spin lock and close the left, this reversal of sequence could easily happen.

Design III, Configuration 3: Final Configuration Testing and Data

The possibility that dud problems previously experienced were caused by the interim spacer being utilized was next addressed. A contract had been previously awarded to a die-cast vendor to supply bodies for the Gearless S&A. The pilot lot submitted was dimensionally incorrect but was reworked by Frankford Arsenal for use in the next ballistic test. Figure 24 shows this final configuration in contrast with the two designs utilized previously. Utilization of this body configuration and a modified rotor spin lock interface resulted in the best test results achieved with the Gearless S&A.

An Arming Distance Test using the 105 mm Howitzer, M2A2, at Zone 7 indicated a mean arming distance at 168.6 ft. (24.5 turns) with a Standard Deviation of 6.1 ft. (0.9 turn). This represented a 1 turn increase in arming delay in comparison with past results using the same design with the interim spacer. Ground Impact tests using the 8 in. Howitzer (M110) at Zone 1 yielded 22 of 24 functions. The remaining two rounds were recovered. In one, the

POST PRESS FIT
INTO LOWER PLATE

POST/BLOCK PRESS FIT
BETWEEN SPACER WALLS
AND DOWELED INTO LOWER PLATE

POST PRESS FIT
INTO SOLID BODY

Figure 24. Spacer/Body Assembly

rotor completed the time delay portion of the arming cycle, and the rotor detonator was initiated but failed to function the lead charge beneath it. In the other the rotor was found having completed 20 of the 23 half oscillations. This was reported as a definite dud. Failure of the rotor detonator to function the lead in the case of the previous round could have been caused by a defective lead charge. The lead was inadvertantly sawed in half upon disassembly and was found to be hollow. This was done with a remote set-up; the possibility exists that the explosive content of the lead spilled out while being sawed. This was not reported as a dud by the Proving Ground.

Table 6 lists the projected arming distance of the Gearless S&A for various weapons and tubes in contrast with the M739 S&A assuming constant turns device. It can be seen that with respect to a 400 caliber non-arm limit, the progressive twist 105 mm Howitzer would be a problem area for both S&A's.

Eccentric Spin Testing

Of the test quantity of forty S&A's fabricated for ballistics, thirty were tested at known predetermined "worst" orientations for various eccentric spin values. The test fixture used was capable of producing eccentric rotation in increments of .015 in. Radial Eccentric Spin Capability (RESC) of these thirty units were distributed as follows:

Orientation	0<RESC<.015	.015<RESC<.030	.030<RESC<.045	.045<RESC<.060
No. of Units	1	2	22	5

Rough Handling Tests

Five of the forty units were subjected to MIL-STD-331 testing sequentially with no setback pins. All forty units of this lot had been run in at 2000 - 3000 rpm upside down after assembly to simulate in-flight bearing surface contact. Testing after each of the rough handling tests were performed in both upside-down and right-side-up orientation to note any deterioration in performance:

1. TV - Procedure I (R&D Phase):

Temperature	No. Units	Results
Ambient	1	Remained safe during test. Able to arm in both orientations at 2000 rpm following test.

Table 6. Arming Distance Comparison – Gearless S&A vs. M739 S&A

WEAPON	Arming Distance (Feet)		Arming Distance (Calibers)	
	GEARLESS	M739	GEARLESS	M739
90mm (M41) Gun	180.8	172.7	612.3	584.8
105mm M2A2 How.	168.8	161.2	490.0	468.0
105mm M103 How.	151.9	145.1	440.9	421.1
4.2 in Mortar	171.5	163.8	490.0	468.0
155mm M109A1 How.	249.2	238.0	490.0	468.0
155mm M1 How.	311.4	297.4	612.3	584.8
175mm Gun	281.3	269	489.9	467.9
8 in. How. M2A1	408.4	390.6	612.6	585.9

1. TV - Procedure I (R&D Phase): (Cont'd)

Temperature	No. Units	Results
-65 F	2	Remained safe during test. Able to arm in both orientations at 2000 rpm following test.
+160 F	2	Both remained safe during test. Both able to arm at 2000 rpm in upside-down orientation. One would not arm in right-side-up orientation.

Internal inspection of all units after this test indicated the presence of a black oily film in areas where metal was in contact with metal during the test. This is generally observed after TV testing with the M125A1 Booster as well and thought to be fretting corrosion usually produced where metals come in contact in a vibrating environment.

Jolt: All units remained safe during this test as required. Spin testing at 2000 rpm after this test indicated the 2 units vibrated hot in the previous test would not arm right-side-up but armed upside-down. The remaining three units armed in both orientations. Internal inspection of all units indicated an increase in the amount of black oily film previously described in bearing areas. Damage was not apparent in any of the five units with the exception of one spin lock leaf spring which deformed slightly but was still operational.

Jumble: A general loosening of internal parts of the M739 fuze was noted after this test; probably due to the fact that both the delay plunger retainer and S&A retainer were not screwed down tight enough. Assembly torque of the delay plunger retainer was not noted but the S&A retainer was assembled with 25 inch pounds of assembly torque which appears to be insufficient. One fuze disassembled completely and spilled the S&A, two retainers, and delay plunger out into the Jumble Box. The S&A in this case came disassembled. S&A movement plate screws had not been staked for this case to facilitate internal inspection after each phase of testing which probably accounts for S&A disassembly.

The remaining four fuzes remained assembled but were loose internally. The S&A's in these fuzes remained safe. Extensive metallic dusting was

observed in these four S&A's due to the smacking of the S&A against the retainer above it. Despite the presence of this foreign matter, two of the four units were able to arm at 2000 rpm in both orientations; the third could arm right-side-up but not upside-down; the fourth partially armed in both orientations.

Explosive Train Testing

Figure 25 illustrates the three basic rotor-escapewheel configurations used in the various designs. In terms of explosive barrier, all three are nearly equivalent since they all expose the .050 in. thick aluminum escapewheel portion of the rotor at some point in the arming cycle. The top rotor assembly (DVA design) provided a .100 in. thick explosive barrier for the first half of the arming cycle but the remaining half only exposed the .050 in. thick escapewheel. The middle design (22% rotor) always exposed the .050 in. thick escapewheel with portions of the cycle where an additional .050 in. brass from the rotor top lamina partially covered the flash hole. The final design (11% rotor) does not utilize a top lamina and therefore, presents an explosive barrier of .050 in. aluminum beneath the flash hole at all times. MIL-STD-1316A requires that "ommission of an interrupter shall not result in a safety failure". This seems to relegate out of line rotors to mere alignment features. However, explosive protection remains a desireable feature from a functional standpoint.

Prototypes

Static Detonator Testing was performed on the first prototypes received from DVA using the M48A3 fuze as a test vehicle.

Phase I. The M24 detonator was initiated in four fuzes containing Gearless S&A's in the fully safe position. Required explosive train interruption was exhibited in all four. The same test was run with S&A's in the half armed position. Again the required explosive train interruption was exhibited. It should be noted here that in this rotor position the only explosive barrier is the .050 in. thick aluminum escapewheel.

Phase II. The M55 detonator in four units was purposely initiated with the rotor in the fully safe position. No damage to the lead charge below was evident. The same test was repeated with four other units in the half armed positioned. Again no damage to the lead charge was apparent.

Engineering Development Quantity

A sample from the 1000 units fabricated by DVA for ED testing were subjected to static detonator tests.

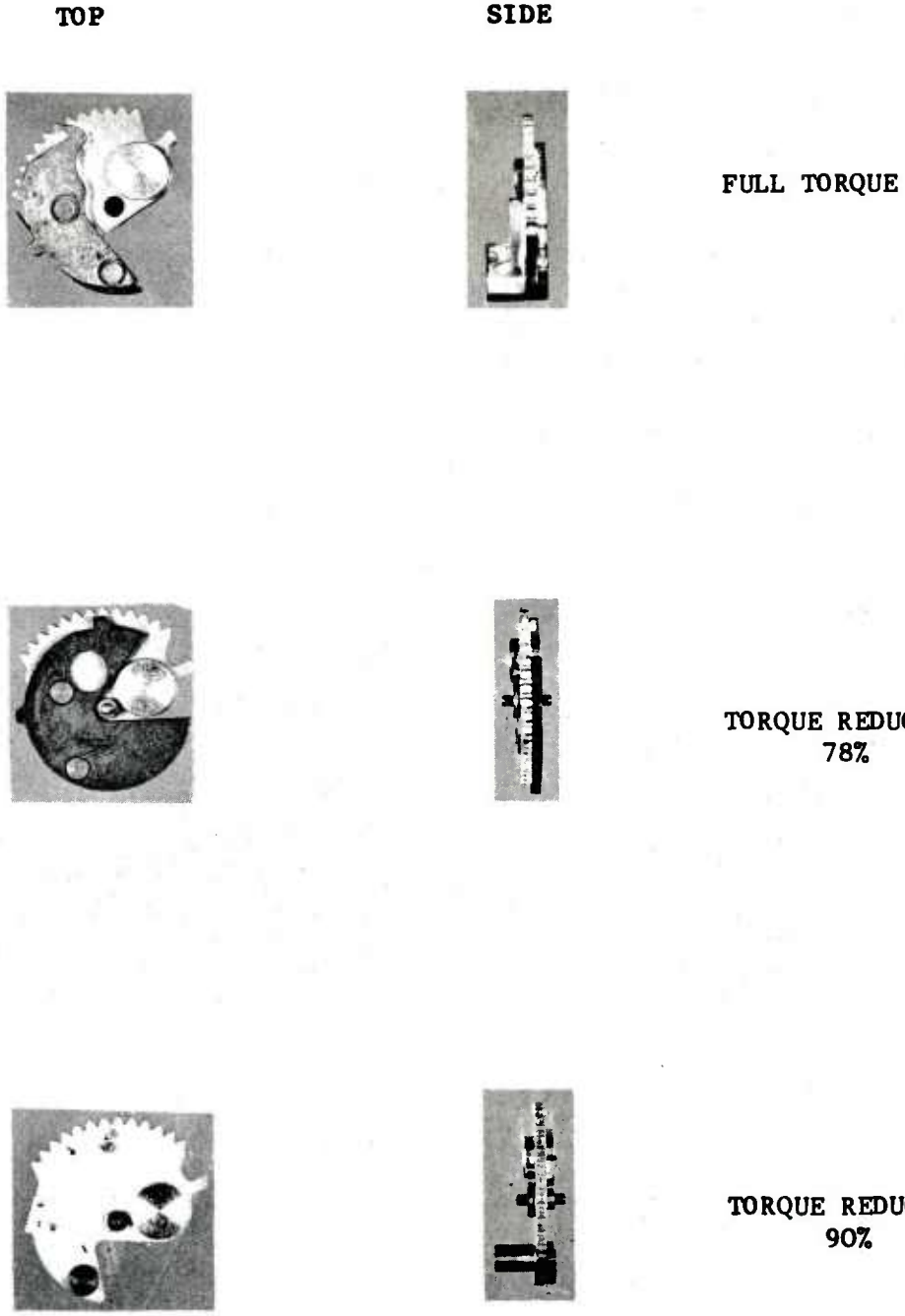

Figure 25. Rotor Gear Assemblies – Gearless S&A

Phase I. Ten units were assembled into M572E2 fuzes in the fully safe position. Fuzes were detonated, and all S&A's provided required explosive train interruption.

Phase II. Ten units were assembled into M572E2 fuzes in the half armed position exposing the .050 in. thick aluminum escapewheel. Fuzes were detonated, and all S&A's provided required explosive train interruption.

A sample of ten units utilizing only the aluminum portion of the rotor-escapewheel as an explosive barrier was tested for static detonator safety. These were assembled into M572E2 fuzes and subsequently initiated. Required explosive train interruption was demonstrated with all units.

The same test as above was repeated with identical hardware preconditioned to -65° F to induce a brittle state in the escapewheel aluminum. Required explosive train interruption was demonstrated with all units.

Tests were run on several samples to determine if an aluminum escapewheel thinner than the .050 in. nominal dimension would induce lead detonation. These were assembled into M572E2 fuzes which were subsequently detonated.

Escapewheel Thickness	Result
.050 in.	Lead Intact. Escapewheel bulged .026 in. beneath blast point but did not break through.
.025 in.	Lead Intact. Escapewheel fractured and pierced by explosive particles which lodged in the escapewheel in the form of a slug.
.013 in.	Same as above.
No Escapewheel	Lead scarred but did not detonate.

General Note: The .050 in. thick rotor-escapewheel has never been observed to be extensively damaged in a static detonator test. The explosive impacting the aluminum escapewheel produces a bulge in the wheel directly below the blast that varies in height from .0 to .014 inches.

More severe rotor damage has been observed on recovered duds wherein impact media (dirt) being forced down the flash hole in addition to the blast of the M24 nose detonator bombards the rotor. The dirt itself has been observed

to be capable of initiating the M17 rotor detonator of the M125A1 booster in recovery tests, and therefore, it must be of a highly energetic nature. This would seriously impair the delay mode operation of the fuze were it not for the fact that the central explosive channel of the fuze is blocked when the fuze is set for "Delay".

In the event that more explosive barrier protection is desired of the Gearless S&A rotor in its final form, an aluminum top lamina design shown in figure 26 exists which effectively doubles the thickness of the barrier underlying the flash hole during the complete arming cycle. This top lamina incorporates the rotor spinlock interface where the spin locks block the rotor and must be riveted onto the escapewheel. This counterbalances the rotor unfavorably and necessitates correction to the escapewheel to correct the rotor cg assembly. The amount and manner of cg correction remains to be determined if a thicker explosive barrier is desired.

Verge Material Studies

The lightweight gearless configurations previously described utilize an aluminum verge made of 7075 T6 Aluminum which is then given a .001 in. thick coating of electroless nickel. Design changes have been made to the verge profile to increase its strength and to reduce the load on the verge faces. The possibility exists that neither the nickel coating nor the stronger alloy aluminum is required. Verges were fabricated using 2024 aluminum made to conform dimensionally to the required configuration usually achieved after nickel coating. The 2024 aluminum was used because it lends itself more readily to progressive die manufacture (especially in the "0" condition).

These verges were assembled onto pallet levers and into Gearless S&A's for tests at Harry Diamond Lab (HDL) on the zero risetime high spin rig. This test equipment has the capability of detenting the rotor gear until the desired spin level (as high as 30,000 rpm) is achieved. The arming time (or turns) of the mechanism is measured at this high spin rate. The following arming delays were reported:

Unit No.	RPM	Arming Delay	Remarks
58	3000	23.96 turns	Baseline reading for comparison purposes.
	6000	26.09 turns	
	20000	26.6 turns	Examination of verge faces showed

ROTOR WITH SOLID
TOP LAMINA

ALTERNATIVE CONFIGURATION

Figure 26. Rotor With Solid Top Lamina and Alternative Configuration

Unit No.	RPM	Arming Delay	Remarks
			dents at point where escapewheel impacts verge faces after "drop" portion of escapement cycle. No tip wear observed on verge or rotor teeth.
	3030	25.62 turns	This reading was taken for comparison with previous low rpm measurement to ascertain effect of any verge distortion on arming delay. A significant deterioration would indicate that the observed wear was of significant consequence.
71	3080	30.88 turns	Baseline reading.
	19730	27.62 turns	Verge faces dented as in previous unit but free of tip wear.
	3000	29.4 turns	
	29000	20.5 turns	Dents in verge faces appeared deeper.
57	3000	26.0 turns	Baseline Reading.
	6030	24.8 turns	
	20000	22.1 turns	Verge faces dented as previously noted. No tip wear evident.
	3000	25.6 turns	
	20000	22.6 turns	
25	3000	27.0 turns	Baseline Reading.
	20000	25.6 turns	Verge faces marked but undented.
	30000	18.5 turns	Verge faces dented.

The above results appear encouraging in that substantial arming delay was still being demonstrated without use of either the nickel coating or stronger alloy aluminum. Future work in this area could result in elimination of the nickel coating (estimated to cost three cents per unit) and utilization of a laminated verge fabricated by using progressive die techniques. The verge utilized in the finalized design is .100 inches thick and coated with .001 inch nickel. This could be divided into three laminates .033 inches thick and left uncoated further reducing the cost of an already inexpensive device when mass produced.

MECHANICS OF THE GEARLESS S&A MECHANISM

1. Friction Not Considered - For a system comprised of two rotational elements in which the first drives the second, a torque applied on the driver is transmitted to the driven member with a magnitude determined by the following relationship: $M = M_d / n$

where M = torque applied to driven gear

M_d = torque on driver

n = gear ratio between the two rotational elements

This equation is true provided: (1) there are no frictional losses either in the first stage or at the mesh where the two elements are in contact; and (2) the gear ratio is constant.

If the second element is reverse biased by some additional means, the net torque on the second element becomes:

$$M_{net} = M - M_b \qquad (2)$$

where M_b = the bias torque

Substituting (1) into (2).

$$M_{net} = (M_d / n) - M_b \qquad (3)$$

Since $M_{net} = I_d \ddot{\Theta}_d$, then

$$I_d \ddot{\Theta}_d = (M_d / n) - M_b \qquad (4)$$

Once again no friction is assumed to exist.

If M_{net} is constant, the motion of the second gear can be described by the following equation:

$$\Theta_d = \dot{\Theta}_o t + (1/2) \ddot{\Theta}_d t^2 \qquad (5)$$

where $\dot{\Theta}_o = \dot{\Theta}_d$ at $t = 0$

Substituting (4) into (5).

$$\Theta_d = \dot{\Theta}_o t + (1/2)t^2 \left[\frac{M_d/n) - M_b}{I_d} \right] (6)$$

The gearless S&A consists mechanically of a large runaway escapement which is essentially one rotational element (the rotor - escapewheel) turning another (the pallet lever). However, the two elements are mechanically intermeshed in such a way that periodically the second element must reverse direction. This inertial reverse is normally enough to bring the driving element's angular velocity to zero or reverse it's direction completely.

The angular velocity vs. time portrait of an escapewheel in a runaway escapement generally appears as in Figure 27 for two half cycles. Phases of Motion I and III are essentially the same with the exception that the wheel drives the pallet lever clockwise in phase I and then counterclockwise in phase III. During phases II and IV the escapewheel is temporarily unlinked from the pallet lever such that it accelerates more rapidly. Generally, Phases II and IV can be considered to contribute little to the overall time delay. If phases I and III are characterized by $\dot{\Theta}_o = 0$, then the half period solution to equation (6) becomes:

$$\tau = \sqrt{\frac{2 I_d \Theta}{(M_d/n) - M_b}} \qquad (7)$$

For the case where the frequency remains constant at a fixed torque level, the total time delay would be:

$$T = O_s \tau \qquad (8)$$

where O_s = number of half oscillations comprising the arming cycle

Observe that the arming time can theoretically be made as high as possible by keeping the denominator in the square root portion close to zero. In reality, this is difficult since the presence of coulomb friction might easily lock the mechanism in such a case. However, it can plainly be seen that the presence of the external bias moment serves to increase the time delay in a controllable fashion. The bias moment in the gearless S&A is generated by centrifugal force and will be discussed later in this report.

Friction Considerations

Mesh Friction

This mesh contact is depicted in figures (3) for entrance and exit

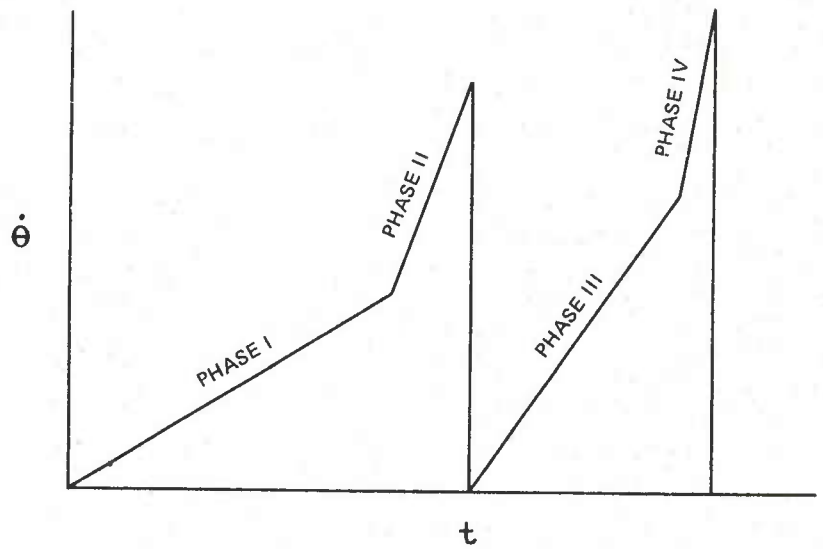

Figure 27. Escapewheel Velocity vs. Time

engagement phases respectively. The sliding of the escapewheel tooth along the verge face creates a frictional force which decreases the amount of torque transmitted to the pallet lever. The torque transmission ratio becomes:

$$\eta^* = A_w^* / A_p^* \qquad (9)$$

These parameters are depicted graphically in Figures (28) and (29). This ratio can be contrasted with the speed ratio given by the following relationship:

$$\eta = A_w / A_p \qquad (10)$$

These are also illustrated in Figures (10) and (11). They are the output and input moment arms respectively of the force which transmits the torque between the two elements.

The angle between the two lines of force LL' and (LL') is related to the coefficient of friction by the relationship:

$$\phi = \tan^{-1} \mu$$

where μ = coefficient of friction

Consideration of mesh friction in the equation of motion serves to change the n in equation (6) to n*, ultimately yielding:

$$T = O_s \sqrt{\frac{2 I_d \Theta}{(M_d / n^*) - M_b}} \qquad (11)$$

Bearing Friction

Centrifugal force and the torque transmission forces generate a side loading on the journals of both the rotor-escapewheel and the pallet lever. A thrust load also exists on the thrust pads of these two parts. In flight, creep acceleration is assumed to move both elements upward toward the movement plate. This loading is generally small in comparison to the radial loads generated by centrifugal force. Assume that the total bearing frictional torque loss is represented by parameters g_r and g_p for the rotor stage and pallet stage respectively. The torque transmitted to the pallet lever in such a case would be:

$$M = (M_d - g_r) / n^* \qquad (12)$$

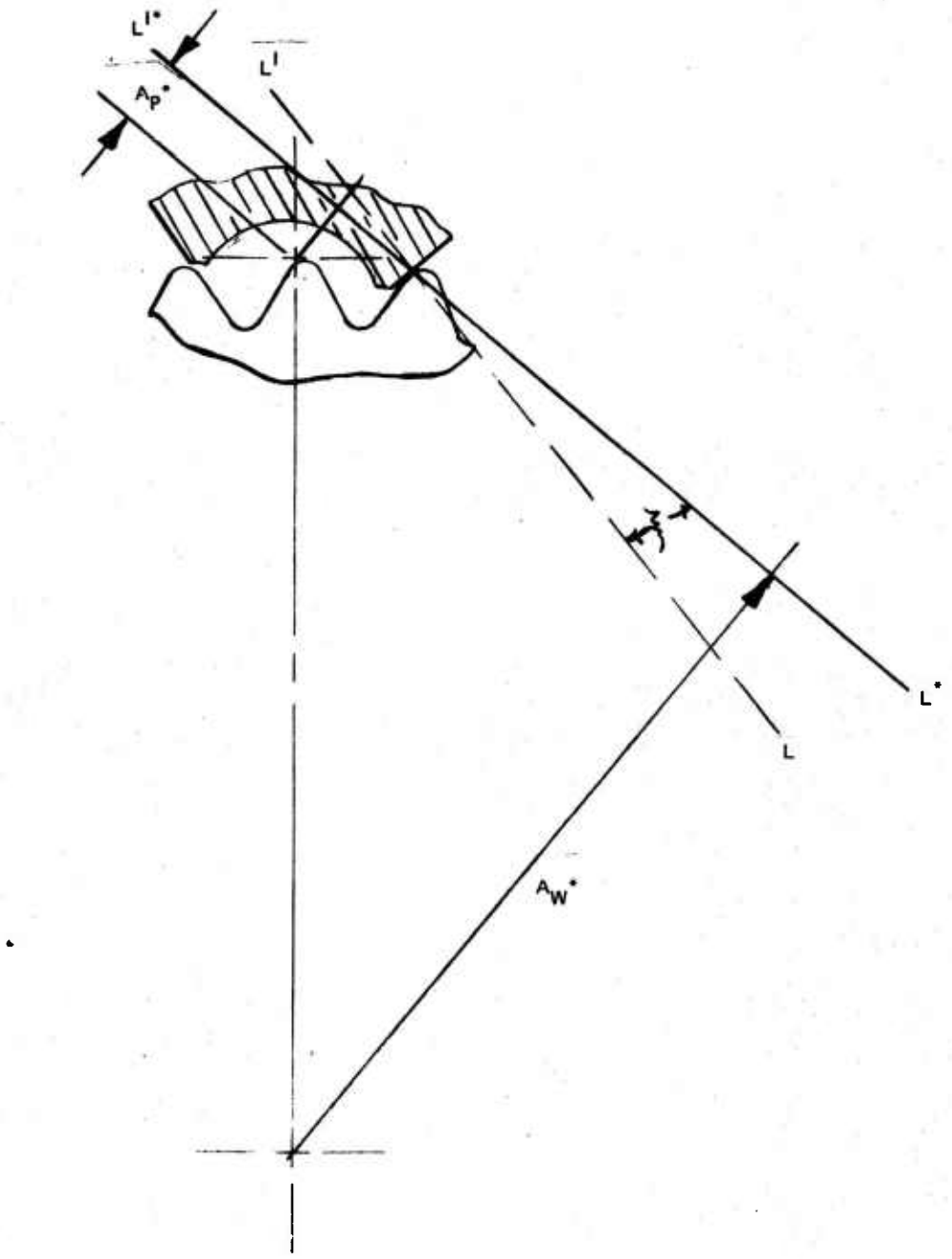

Figure 28. Friction Modified Moment Arms – Entrance Engagement

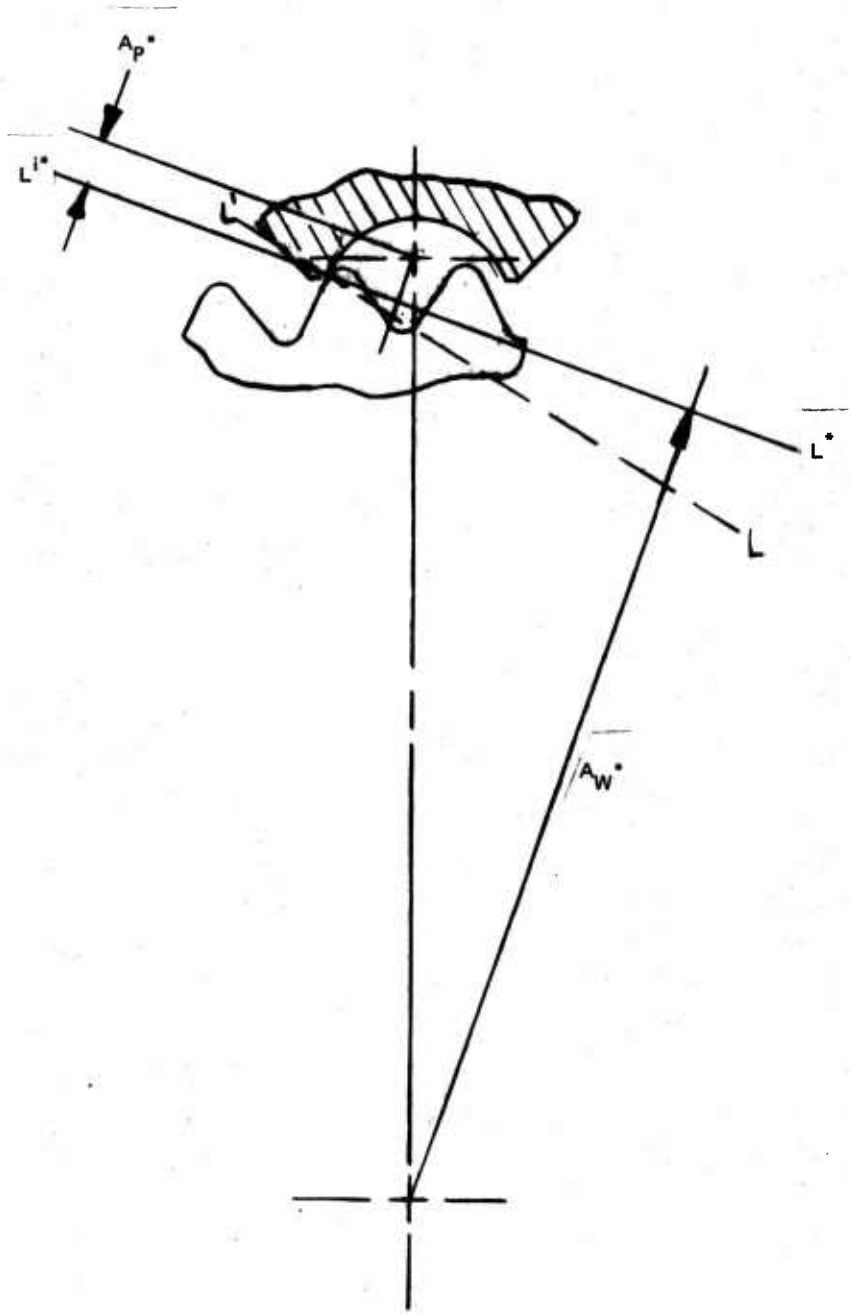

Figure 29. Friction Modified Moment Arms – Exit Engagement

The net torque on the lever would then be:

$$M_{net} = \left[(M_d - g_r)/n^*\right] - M_b - g_p \qquad (13)$$

The total arming time would then become:

$$T = O_s \sqrt{\frac{2 I_p \Theta}{\left\{\left[M_d - g_r\right]/n^*\right\} - M_b - g_p}} \qquad (14)$$

It can be seen that bearing losses can be quite significant, especially that of the pallet lever. One must realize that if the denominator ever goes to zero and this zero net torque condition remains, the system approaches a lock up and will jam once the kinetic energy of the parts is expended. Angular momentum of the parts may carry them through engagement positions in which the zero net torque condition prevails, so the escapement may not jam. However, this situation should be avoided due to the highly variable nature of coulomb friction.

Other System Variables

Equation (14) takes into account all realistic system variables with the exception of the following:

1. rotor inertia
2. fluctuating linkage ratio
3. fluctuating input torque
4. fluctuating external bias torque
5. dynamic effects introduced by pivot clearances

These will be discussed herein but need not be considered for redesign guidelines.

Rotor Inertia

One can take an alternate approach to computing the arming delay which yields essentially the same result as equation (14) but takes into account rotor inertia. In this approach, the focus is on rotor motion.

If one applies a moment on a single rotational element, in this case the rotor, it will angularly accelerate according to Newton's second law in rotational form:

$$M = I_R \ddot{\Theta}_R \qquad (15)$$

If the rotational element is geared to another rotational element, however, the equation becomes:

$$M = \left[I_R + n^2 I_p \right] \ddot{\Theta}_R \qquad (16)$$

where n = gear ratio (or linkage ratio) between the two elements.

Coulomb friction in the gear mesh changes this equation to the following:

$$M = \left[I_R + nn^* I_p \right] \ddot{\Theta}_R \qquad (17)$$

where n* = ratio of friction modified moment arms discussed previously.

Coulomb friction in the bearings which bring about frictional torque losses g_r and g_p in the bearings of the rotor and lever respectively change the previous equation as follows:

$$M - (g_r + n^* g_p) = \left[I_R + nn^* I_p \right] \ddot{\Theta}_R \qquad (18)$$

Lastly, some additional bias torque acting on the lever changes the equation to the following:

$$M - n^* M_b - (g_r + n^* g_p) = \left[I_R + nn^* I_p \right] \ddot{\Theta}_R \qquad (19)$$

One can interpret the effect of the linkage between the two parts as one of magnification. The lever's inertia is magnified by at least the square of the linkage ratio while the frictional bearing torque and lever bias is magnified by at least the first power of the linkage ratio.

Again assuming constant angular acceleration of the two rotating members within one half oscillation, the period of the half oscillation can be obtained from equation (19) and the following results:

$$\tau = \sqrt{\frac{2 \left[I_R + nn^* I_p \right] (\Delta\Theta_R)}{M - n^* M_b - (g_r + n^* g_p)}} \qquad (20)$$

Similarly the total arming time becomes:

$$T = O_s \sqrt{\frac{2\left[I_R + nn^* I_p\right](\Delta\Theta_R)}{M - n^* M_b - (g_r + n^* g_p)}} \qquad (21)$$

This reduces to equation (14) for the case where $nn^* I_p$ is approximately equal to $I_R + nn^* I_p$ when one realizes that $(\Delta\Theta_R) = \Theta_{p/n}$

The term nn^* for the gearless mechanism is numerically on the order of 50 to 150. Since the polar inertias of the rotor and lever are roughly equal, it can be seen that the rotor's inertial figures little in the determination of the period of the half oscillation. However the rotor's inertia can be important in determining both the dynamic oscillation angle and the impact velocity of the two parts on re-engagement. This last factor affects the dynamic loading on both the escapewheel teeth and verge faces.

Linkage Ratio Fluctuation

The entrance and exit linkage ratios for this device are illustrated in Figure 12. One can see that they are not constant but change as the lever oscillates. This is not unusual for an escapement mesh and is even common for clock gear meshes. In contrast, the involute gear mesh provides a theoretically constant linkage or gear ratio, but here too the changing mesh efficiency results in a variable torque transmission introducing similar difficulties in solving the differential equation of motion of the moving parts.

A useful alternative is to make some mathematical approximation of an average value and then consider the linkage ratio as being constant for each half cycle. The time delay should be computed seperately for each.

Input Torque Variation

Within any half oscillation the variation in input torque can be considered small. The output torque of the rotor gear is given by the following:

$$\text{Torque} = \left[\frac{W}{g} R_s R_p \sin \phi_R\right] w^2$$

where W=weight of rotor gear

R_s = distance from rotor pivot to rotor c. g.

R_p = distance from spin center to rotor pivot

ϕ_R = included angle between R_s and R_p.

w = spin rate of the projectile

The geometrical parameters are illustrated in Figure 30.

The angle ϕ_R varies from 45° to 135° increasing approximately four degrees each half oscillation. Approximately two of the four degrees is expended during the "drop" portions of escapement motion. Within any half oscillation, then, one can expect a maximum torque increase of 3.4% (first half cycle) and a maximum torque decrease of 3.3% (last half cycle). Figure 31 illustrates the range of torque variation to be expected for each half cycle.

It can be seen that while the torque does fluctuate throughout the entire arming cycle, it fluctuates little within any half cycle. Little error would be introduced in the arming time calculation if each half period is computed separately assuming constant torque for that half cycle.

Fluctuating External bias on pallet lever

The pallet lever assembly is purposely unbalanced with respect to its own axis of rotation. This unbalance creates a turning moment in a centrifugal force field which at times opposes the direction of lever rotation and at times assists the rotation of the lever. The c.g. of the lever assembly is radially offset approximately .010 from the pivot in a direction toward the spin center. This is illustrated in Figure 32. In its furthest position of oscillation, it offers the most resistance to rotation; but as the lever is moved toward "dead" center (c.g. aligned with centrifugal force vector), less opposition to rotation is offered. As the c.g. flips passed dead center, centrifugal force begins driving the lever to the opposite extreme of its oscillation. This moment or bias can be computed using the same formula derived for torque on centrifugal gears:

$$M_b = mw^2 r_s r_p \sin \psi \qquad (23)$$

where m = mass of lever assembly

w = spin rate of projectile

r_s = c.g. offset from lever pivot

r_p = pivot offset from spin axis

ψ = included angle between r_s and r_p.

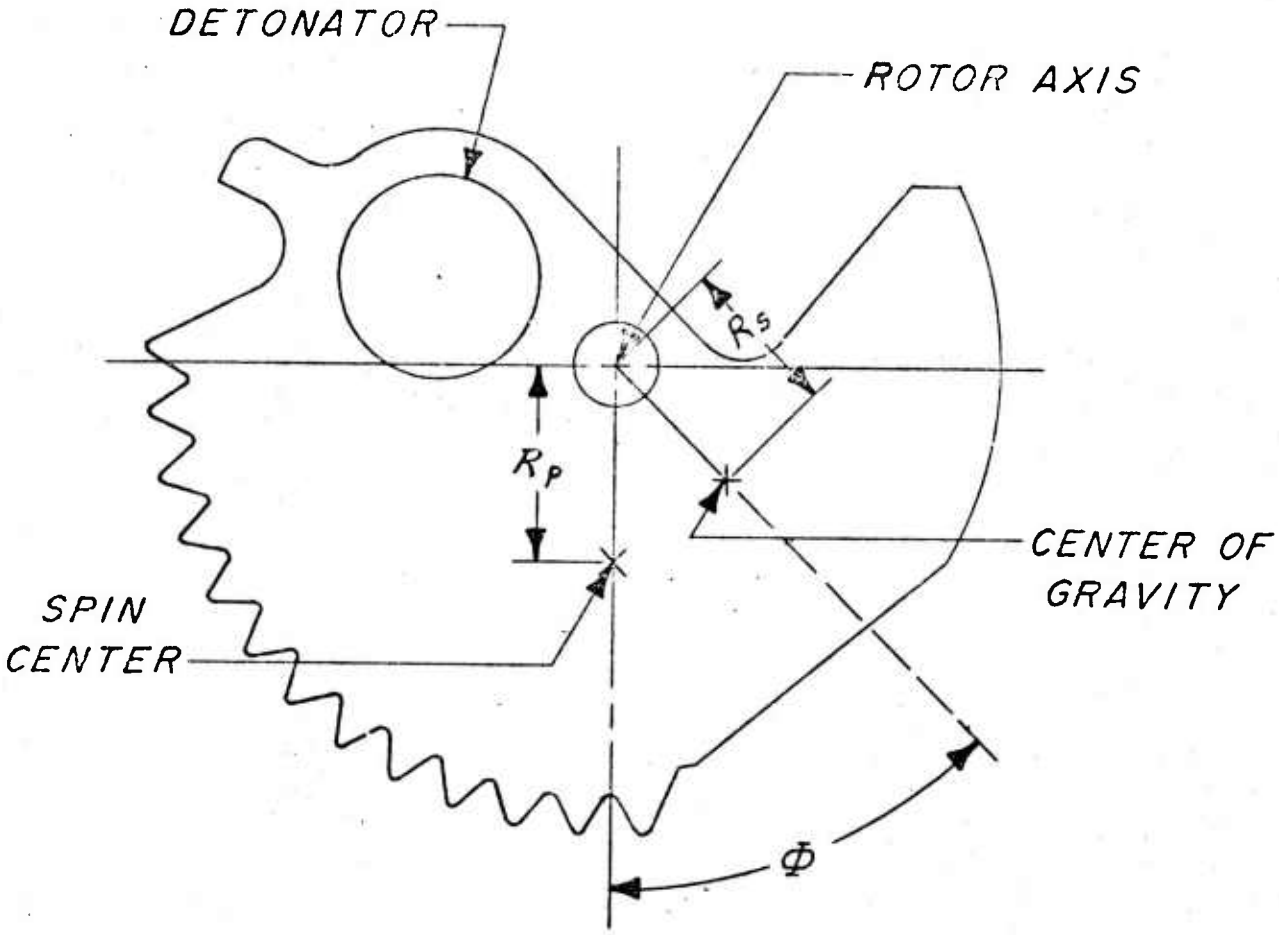

Figure 30. Rotor Torque Parameters – Start Position

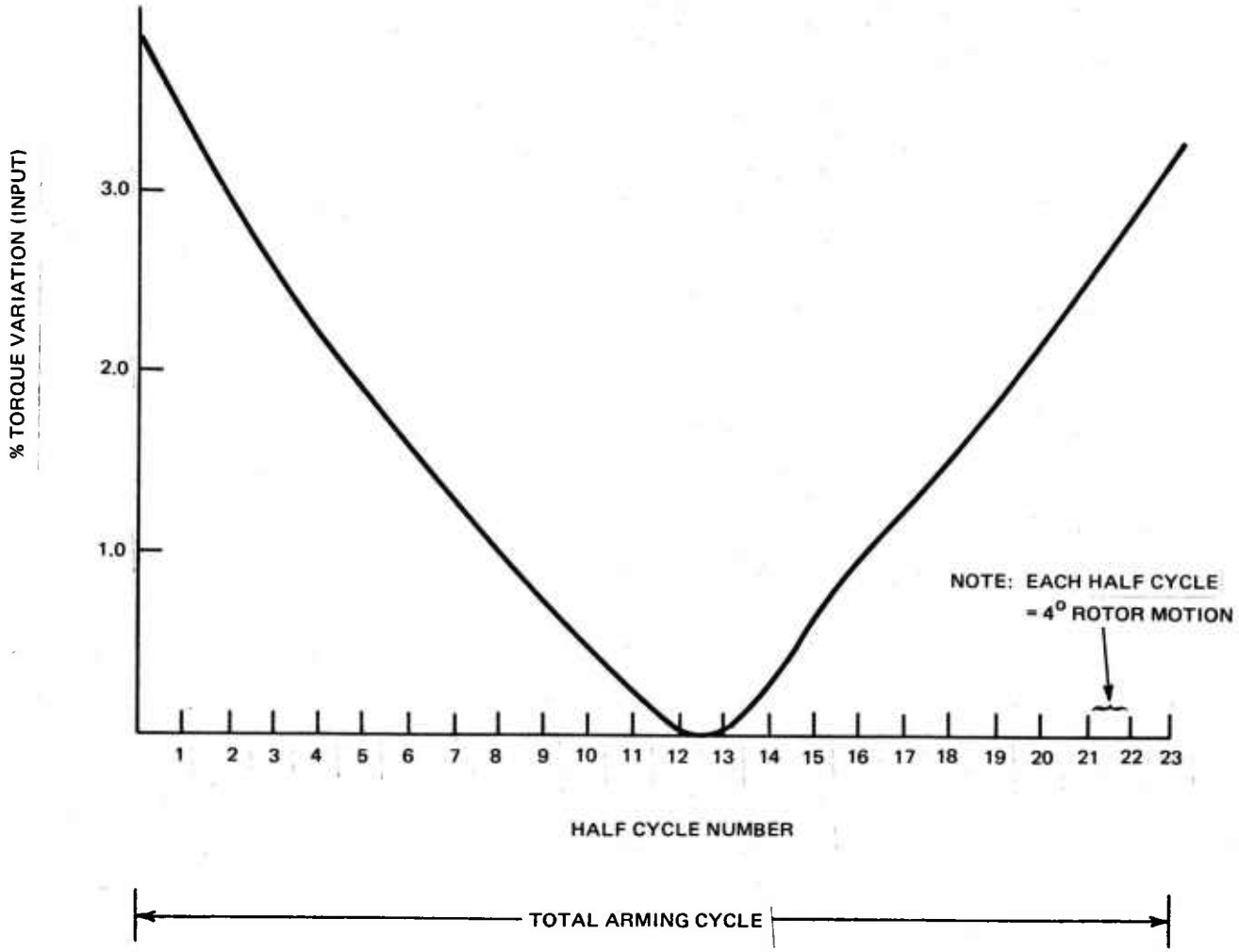

Figure 31. Torque Variation vs. Rotor Position

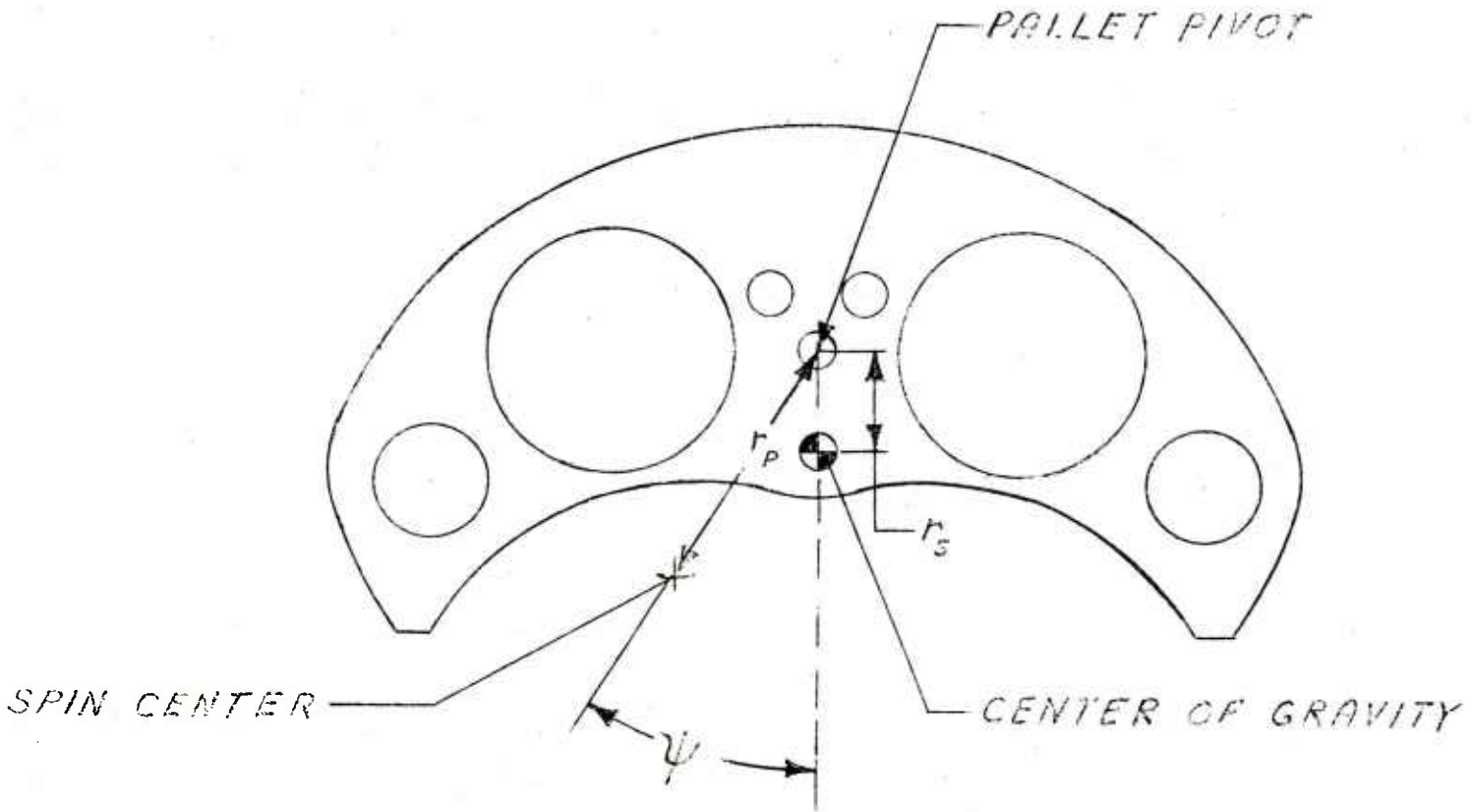

Figure 32. Pallet Lever Torque Parameters

Figure 32 illustrates r_s, r_p, and angle ψ as they relate to the lever's pivotal postion. Notice that the rotor and lever pivots are located diametrically opposite one another with respect to the spin center. Overall an angle of oscillation of the lever approximately equal to 2ψ results. During any half cycle the lever will oscillate from approximately +10° to -10°. Inserting this range of ψ into equation (23) indicates that for the first half of the cycle, the lever opposes the rotor; while in the second half of each half cycle the lever cooperates with the rotor. With this being the case, the question arises here whether or not the net effect of the lever unbalance is not zero.

The answer to this question may be that the net effect would be zero if the escapement linkage ratio were either constant or symmetrical with respect to the $\psi = 0$ orientation. But in reality, the linkage ratio (shown in figure 12) tails off badly for the second portion of each half cycle. The net result is a low net applied torque for the $\psi < 0$ portion of the half cycle and a high applied torque for the $\psi > 0$ portion of the half cycle. The c.g. orientation as such also tends to index the verge face further into the root of the next tooth increasing the lever's angle of oscillation which is important in determining the half period of oscillation.

Effects Induced By Pivot Clearances

One effect of pivot clearance is related to computation of the frictional torque loss in the escapement's bearings. It is well known that a cylindrical member such as a pivot rotating in a hole tends to seek a steady state position as shown in Figure 33, where the angle λ is given by $\lambda = \tan^{-1}\mu$.

where = coefficient of friction between the two contacting surfaces.

The frictional torque loss, assuming boundary lubrication, is computed by the formula:

$$g_o = p r \sin(\tan^{-1}\mu) \qquad (24)$$

where p = load

r = journal radius

μ = coef. of friction

It is apparent that if the pivot were not rotating it would rest at the bottom of the hole. Likewise, if it were rotating in the opposite direction it would rest at an angle minus λ. Remember that the lever reverses direction of rotation

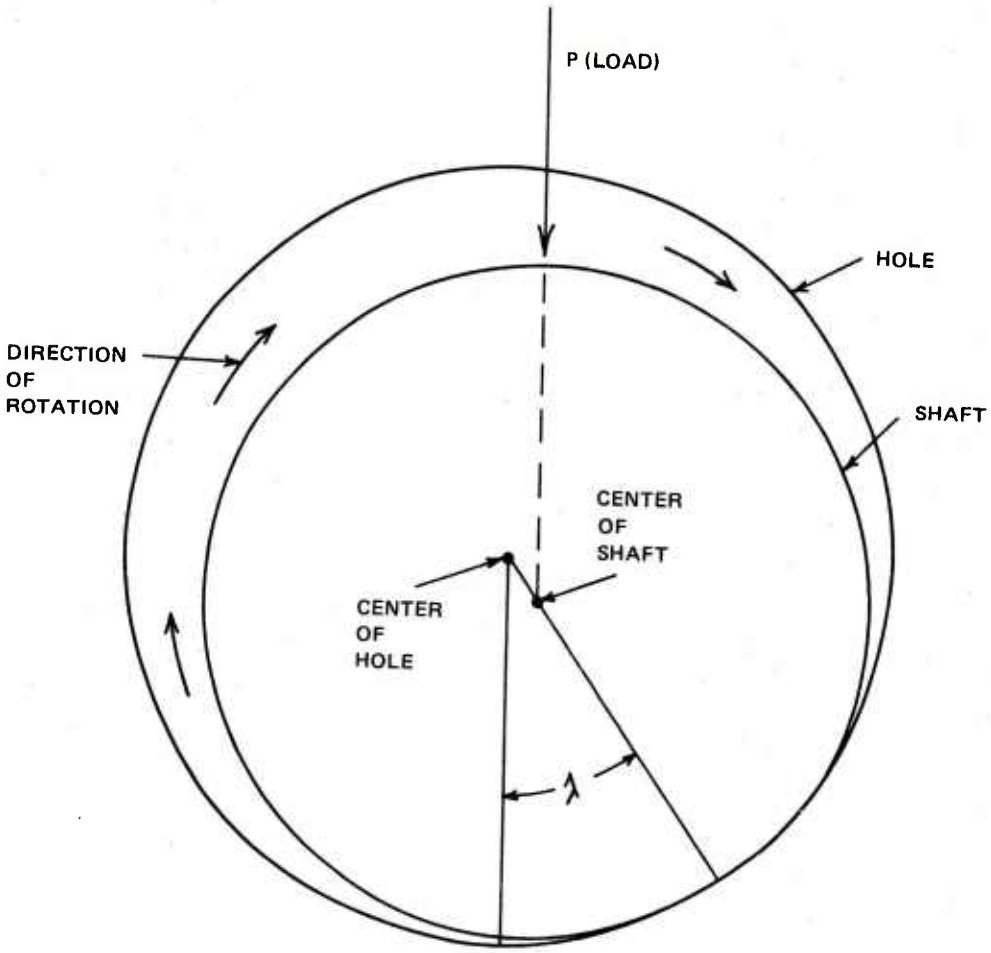

Figure 33. Steady-State Journal Position In Hole

twice each cycle indicating an inherent tendency for the pivot to change position in the hole each time it must reverse its direction of rotation. It should be clear that the frictional torque loss between the times when the steady state positions at $\pm\lambda$ are achieved will not correspond to that computed in equation (24) for steady state conditions. Pure rolling without slipping may or may not occur depending on many physical parameters of the system - one of which is the diametral pivot clearance.

The minimum diametral clearance generally designed into devices of this nature is .001 in. which only occurs when the largest journal diameter permitted is combined with the smallest pivot hole permitted. Typical clearance for parts at mean dimensions is .002 in.

Turns-To-Arm

The question arises whether this gearless device will exhibit a constant turns-to-arm with respect to spin rate of the projectile. The turns-to-arm characteristic observed with other S&A's for spin stabilized artillery comes about because the runaway escapement's resistance to drive force is proportional to the square of the speed at which the rotor moves. The fact that the pallet lever's unbalance moment is proportional to the square of the projectile's spin rate preserves the desired turns-to-arm characteristic. This can be shown as follows:

Starting with equation (7), the expression for the period of the half oscillation, we can substitute equations (22) and (23) which yields:

$$\tau_{1/2} = \sqrt{\frac{2\left[I_R + nn^* I_p\right](\Delta\phi)}{\frac{W}{g}\omega^2 R_s R_p \sin\phi - n^*\frac{w}{g}\omega^2 r_s r_p \sin\psi - (g_r + n^* g_p)}} \tag{25}$$

The bearing loss terms g_r and g_p can be broken up into two components, one representing centrifugal losses and the other thrust losses, i.e.

$$g_r = B_r \omega^2 + \alpha_R \tag{26}$$

$$g_p = B_p \omega^2 + \alpha_P \tag{27}$$

Substituting equations (26) and (27) into (25), we obtain:

$$\tau_{1/2} = \sqrt{\frac{2\left[I_R + nn^* I_p\right](\Delta\phi)}{\frac{W}{g}\omega^2 R_s R_p \sin\phi - n^*\frac{w}{g}\omega^2 r_s r_p \sin\psi - (B_r + n^* B_p)\omega^2 - (\alpha_R + n^*\alpha_p)}} \tag{28}$$

We can now factor out the ω from the denominator:

$$\tau\ 1/2 = \frac{1}{\omega}\sqrt{\frac{2\left[I_R + nn^* I_p\right](\Delta\phi)}{\frac{W}{g}R_s R_p \sin\phi - n^*\frac{w}{g}r_s r_p \sin\psi - (B_r + n^* B_p) - \left[(\alpha_r + n^*\alpha_p)/\omega^2\right]}} \tag{29}$$

Since the number of revolutions of the projectile in time duration $\tau_{1/2}$ is $N_{1/2} = \frac{1}{2\pi}\omega\tau_{1/2}$, we have, on substituting equation (20) into this relationship:

$$N_{1/2} = \frac{1}{2\pi}\sqrt{\frac{2\left[I_R + nn^* I_p\right](\Delta\phi)}{\frac{W}{g}R_s R_p \sin\phi - n^*\frac{w}{g}r_s r_p \sin\ - (B_r + n^* B_p) - \left[(\alpha_r + n^*\alpha_p)/\omega^2\right]}} \tag{30}$$

Note that the expression is independent of ω except for the final term in the denominator representing the thrust load losses. One can see two cases where this term becomes insignificant:

(1) where the coefficient of friction on the thrust surfaces is zero making the terms zero.

(2) where ω is large enough that the value of the denominator in equation (30) is hardly changed by including this last term.

A graph of N vs. ω appears as in Figure 34.

The flat portion of the curve is indicative of a true double integrating device. One can then see that this particular gearless device should exhibit a constant turns-to-arm provided the appropriate range of spin rates are considered.

Mechanism Redesign

The original gearless S&A device design was shown to be structurally unsound in the areas of the escapement mesh and pallet pivot. This resulted in premature arming of the mechanism in both the 19.5 krpm environment of the 90 mm Gun and the 13.5 krpm environment of the 105 mm Howitzer. One approach taken to eliminate these structural defects was to decrease the loading both on the pivots and on the mesh surfaces. The following shows how this can be done and what guidelines to follow during redesign to achieve the desired time delay without structural failure.

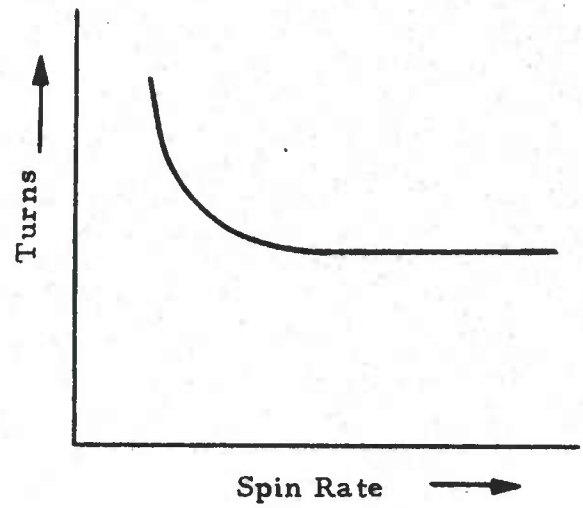

Figure 34. Turns-to-Arm vs. Mechanism Spin Rate

The redesign objective is to contrive a similar gearless device which provides nearly the same time delay at high rpm that the structurally deficient device provided at low rpm. This new device should operate at high rpm without resulting in structural damage and should likewise be capable of arming readily at low rpm as well. It is assumed that reducing the loading on the lever's pivots and escapement's mesh surfaces will eliminate structural failure.

If for each half oscillation the period is preserved, then the total arming time of the device should be preserved as long as the number of half cycles remains unchanged. In terms of equation (29) the objective becomes to make:

$$\tau^*_{1/2} / \tau_{1/2} = 1$$

Where $\tau^*_{1/2}$ represents the period of half oscillation of the lever in the new device; $\tau_{1/2}$ represents the period of half oscillation of the lever in the original device.

Equation (29) is rewritten here for convenience:

$$\tau_{1/2} = \frac{1}{\omega} \sqrt{\frac{2\left[I_R + nn^* I_p\right](\Delta\phi)}{\frac{W}{g} R_s R_p \sin\phi - n^* \frac{W}{g} r_s r_p \sin\psi - (B_r + n^* B_p) - \left[(\alpha_r + n^* \alpha_p)/w^2\right]}}$$

Observe that $\delta^*_{1/2}$ can be made equal to $\tau_{1/2}$ if the numerator and demoninator of equation (29) can be changed such that

$$(\text{Numerator})^* = \delta \text{ Numerator}$$

$$(\text{Denominator})^* = \delta \text{ Denominator}$$

Observe that the δ cancels out the fraction and the $\tau_{1/2} = \tau^*_{1/2}$ objective is attained. This can be done physically as follows:

Denominator:

1. Construct a new rotor gear whose output torque is reduced by a factor of $(1-\delta)$. This will result in loading which similarly is reduced by a factor of $(1-\delta)$. It was observed that a $\delta = .22$ was sufficient to eliminate structural failure in the escapement mesh.

2. Construct a new pallet lever whose unbalance moment as computed by equation (23) is reduced such that the unbalance moment of the new lever is equal to δ times the unbalance moment of the old design.

3. The linkage ratio can be preserved through either scaling all length dimensions of the escapement up or down as desired, or by preserving the overall geometrical configuration of the escapement. This can be done even though the parts are made lighter.

4. Design the lever such that bearing loss in the redesign equal δ times the bearing losses of the old design. This can be done by reducing the lever's weight, reducing the lever's pivot diameter, or by reducing the lever's pivotal offset from the spin center. Any one of these or combination thereof can be used to achieve the desired objective.

Adhering to suggestions 1 through 4 will result in a mechanism in which the net torque on both the rotor and lever will be reduced by a factor of $(1 - \delta)$.

Numerator:

5. Construct a rotor gear whose polar moment of inertia is equal to δ times the old moment of inertia. It was shown previously how rotor inertia little affects arming time. But observe that suggestion 1, dealing with rotor output torque, is also affected by factors one would adjust to change rotor inertia.

6. Construct a lever whose polar moment of inertia is equal to δ times that of the old lever. Note that this must be done simultaneously while following suggestion 2 dealing with the lever unbalance parameters.

7. Maintain the same angle of oscillation in the new design as in the old.

General Comment

It should be apparent that suggestions 1 through 7 are not the only way to achieve the desired objective. These appeared easiest, however, considering spatial constraints which existed. The advantage of following these seven suggestions are that the friction sensitivity of the device should in no way be compromised.

SUMMARY

The program conducted to date and summarized herein indicates that a Gearless Safe and Arming Device for Artillery Fuzing is technically feasible. The device which evolved after numerous configuration changes prompted by field testing and engineering analysis is rugged, small in size, potentially inexpensive, and capable of meeting desired arm-non arm requirements. The

few disadvantages expected to be associated with the absence of a gear train from a structural standpoint have been resolved resulting in a mechanism capable of withstanding the extreme environments of large caliber weapon systems.

RECOMMENDATIONS

The device described and tested herein merits consideration for further development and testing. It's small size permits almost direct interchangeability with the current M739 and XM587 S&A's. Being smaller than the M125A1 Booster Module, it can be used in the M557, M572, and M564 Fuzes. It can also replace the M577 SSD and M732 S&A as well. The absence of a gear train and hobbed pinions would relieve a serious mobilization burden and potentially eliminate precision pinions entirely from safe and arming devices for artillery fuzing.

GLOSSARY

A_p	input moment arm of driven element
A_w	output moment arm of driving element
A_p^*	friction adjusted input moment arm of driven element
A_w^*	friction adjusted output moment arm of driving element
F_w	force exerted by escapewheel
g	gravitational acceleration
g_o	journal bearing torque loss
g_p	bearing loss in pallet lever stage
g_r	bearing loss in rotor stage
I_d	polar inertia of driven element
I_p	polar inertia of pallet lever
I_r	Polar inertia of rotor wheel
m	mass of pallet lever
M	torque applied to driven element
M_b	bias torque
M_d	torque on driving gear
M_{net}	net torque on driven element
n	angular velocity ratio between two rotational elements
n*	friction adjusted torque ratio
N	number of turns

GLOSSARY CONTINUED

O_s	number of half oscillations
P	net load on journal
r	journal radius
r_p	distance from spin center to lever pivot
r_s	distance from lever pivot to lever c. g.
R_p	distance from spin center to rotor pivot
R_s	distance from rotor pivot to rotor c. g.
t	time
T	total arming time
w	weight of pallet lever
z	cross section verge thickness
α_p	pallet lever bearing loss invariant with spin rate
α_r	rotor bearing loss invariant with spin rate
B_p	pallet lever bearing loss constant relating frictional torque loss and w^2
B_r	rotor bearing loss constant relating frictional torque loss and w^2
ϕ_r	included angle between R_s and R_p
λ	angle between bottom of hole and steady slate position of journal in the hole
μ	coefficient of friction
w	spin rate of projectile
τ	half period

θ	angular rotation
$\ddot{\theta}$	angular acceleration
θ_d	angular displacement of driven element
$\dot{\theta}_d$	angular velocity of driven element
$\ddot{\theta}_d$	angular acceleration of driven element
θ_o	initial angular velocity
θ_r	angular acceleration of rotor wheel
ψ	included angle between r_s and r_p
γ	friction angle

DISTRIBUTION LIST

Commander
U.S. Army Armaments Command
Rock Island, IL 61201

1 Attn: DRSAR-RD-F,
W. Benson

1 Attn: DRSAR-RD-F,
J. Sagarese

1 Attn: DRSAR-RD-K,
B. Kmech

1 Attn: DRSAR-RD-K,
G. Taylor

1 Attn: DRSAR-RD-F,
Col. Mueller

Commander
US Army Materiel Development and
Readiness Command
Attn: DRCDE-WC
5001 Eisenhower Avenue
Alexandria, VA 22333

Commander
Harry Diamond Laboratories
2800 Powder Mill Road
Adelphia, MD 20783

1 Attn: AMXDO-TIB
1 Attn: R. Ebner Br. 420,
1 Attn: Br. 420,
D. Overman

1 Attn: Br. 420,
R. Johnson

National Academy of Science
Materials Advisory Board
Attn: Dr. J.R. Lane
2101 Constitution Avenue, N.W.
Washington, DC 20418

City College of New York
Mech. Eng. Dept.
Attn: Prof. G. Lowen
137th Street & Convent Avenue
New York, NY 10031

Commander
Picatinny Arsenal
Dover, NJ 07801

1 Attn: SARPA-AD-F,
F. Saxe

1 Attn: SARPA-AD-F-E,
A. Nash

1 Attn: SARPA-AD-F-E-1,
E. Stearns

1 Attn: SARPA-AD-F-E-4,
D. Taravella

1 Attn: SARPA-AD-F-E-D,
D. Popovitch

1 Attn: SARPA-AD-F-E-D,
B. Schulman

1 Attn: SARPA-ADED,
L. Post

1 Attn: SARPA-ADED,
M. Wiener

1 Attn: SARPA-ADED,
E. Entin

1 Attn: SARPA-ADED,
W. Pellet

1 Attn: SARPA-ADED,
H. Hoganson

1 Attn: SARPA-AD-F-D,
R. Brennan

1 Attn: SARPA-AD-F-D,
T. Tese

1 Attn: SARPA-AD-F-D,
F. Tepper

Commander
Technical Library, Bldg 313
Aberdeen Proving Ground, MD
21005

DISTRIBUTION LIST (Contd)

Commander
AF Armament Laboratories
Attn: DLOS
Eglin AFB, FL 32542

Defense Documentation Center (12)
Cameron Station
Alexandria, VA 22314

Frankford Arsenal:

1 Attn: AOA-M

1 Attn: TD

1 Attn: PA

1 Attn: PD
Mr. Geo. White

1 Attn: GC

1 Attn: QAA-R

1 Attn: MDA-E
E. J. Ramsay

1 Attn: MDA-E
F. Schad

1 Attn: MDA-E
H. Freels

1 Attn: MDA-E
C. Cuprys

1 Attn: MDA-E
W.W. Lordan

1 Attn: MDA-R
D. Lenton

1 Attn: MDA-R
K. Ryan

1 Attn: MDA-R
R. Tramo

1 Attn: PDM-E
P. Gordon

Frankford Arsenal (Cont'd)

1 Attn: TSE-E
H. Goldman

1 Attn: MTT-E
R. Giordano

1 Attn: MTM
D. Reap

1 Attn: PDC
J. Messina

3 Attn: TSP-L/51-2
(1 - Reference copy,
1 - Circulation copy,
1 - Record copy)

Printing & Reproduction Division
FRANKFORD ARSENAL
Date Printed: 20 March 1975